



EUROPEAN  
COMMISSION

European  
Research Area

# Carbon-14 Source Term

## CAST



## Knowledge supporting Safety Assessments of $^{14}\text{C}$ (D6.2)

Capouet M., D. Boulanger, T. Vandoorne, R. Gaggiano (ONDRAF/NIRAS), S. Norris, S. Williams (RWM), S. Schumacher (ANDRA), A. Rübél (GRS), O. Nummi (FORTUM), P. Poskas, A. Narkuniene, D. Grigaliuniene (LEI), A. Vokál (SURAO), J. Mibus (NAGRA), E. Rosca-Bocancea, J. Hart (NRG), B. Ferrucci, R. Levizzari, A. Luce (ENEA), D. Diaconu (RATEN ICN), M. Cuñado Peralta (ENRESA), H. Owada (RWMC), B. Kienzler (INE/KIT), E. Wieland, L. Van Loon (PSI) and R. Walke (QUINTESSA).





EUROPEAN  
COMMISSION

European  
Research Area

Date of issue of this report: 21/04/2017

<b>The project has received funding from the European Union's Seventh Framework Programme for research, technological development and demonstration under grant agreement no. 604779, the CAST project.</b>		
<b>Dissemination Level</b>		
<b>PU</b>	Public	<b>x</b>
<b>RE</b>	Restricted to the partners of the CAST project	
<b>CO</b>	Confidential, only for specific distribution list defined on this document	



## ***CAST – Project Overview***

The CAST project (CARbon-14 Source Term) aims to develop understanding of the potential release mechanisms of carbon-14 from radioactive waste materials under conditions relevant to waste packaging and disposal to underground geological disposal facilities. The project focuses on the release of carbon-14 as dissolved and gaseous species from irradiated metals (steels, Zircalloys), irradiated graphite and from ion-exchange materials.

The CAST consortium brings together 33 partners with a range of skills and competencies in the management of radioactive wastes containing carbon-14, geological disposal research, safety case development and experimental work on gas generation. The consortium consists of national waste management organisations, research institutes, universities and commercial organisations.

The objectives of the CAST project are to gain new scientific understanding of the rate of release of carbon-14 from the corrosion of irradiated steels and Zircalloys and from the leaching of ion-exchange resins and irradiated graphites under geological disposal conditions, its speciation and how these relate to carbon-14 inventory and aqueous conditions. These results will be evaluated in the context of national safety assessments and disseminated to interested stakeholders. The new understanding should be of relevance to national safety assessment stakeholders and will also provide an opportunity for training for early career researchers.

For more information, please visit the CAST website at:

<http://www.projectcast.eu>

CAST		
Work Package: WP6	CAST Document no. :	Document type: R
Task: 6.2	CAST-2016-D6.2	R = report, O = other
Issued by: ONDRAF/NIRAS		Document status: Final
		Draft/Review/Final

Document title
Knowledge supporting Safety Assessments of <sup>14</sup> C

## Executive Summary

Work Package 6 of the CAST project is devoted to the knowledge base concerning the release and transport of <sup>14</sup>C in the context of post-closure safety assessments of the geological disposal of radioactive waste. This report (D6.2) assesses the various approaches for safety assessment discussed in report D6.1 in the light of the existing knowledge about the <sup>14</sup>C source term. It proposes a synthesis of D6.1, identifies commonalities and differences between approaches and concepts and highlights safety-critical uncertainties pertaining to <sup>14</sup>C fate in waste disposal.

Past long-term safety assessments show that speciation of <sup>14</sup>C is crucial for the determination of its radiological impact. As inorganic, <sup>14</sup>C provides good retention capabilities in cement (that usually makes the EBS of ILW/LLW repository) and in clay. However, as organic, <sup>14</sup>C is considered not retarded or very weakly in safety assessment giving rise to a more pronounced radiological impact. <sup>14</sup>C is usually not a concern for high level waste (spent fuel assemblies and vitrified waste) because of the containment requirement and/or the good stability (slow release) of the waste matrix.

At mid-term of the project, a review of the CAST reports providing a state-of-art of <sup>14</sup>C knowledge for the four waste materials and its abstraction in safety assessment (D2.1, D3.1, D1.4, D5.5, D6.1), as well as the preliminary experimental results available has been carried out. The following points of interest for safety assessment can be derived.

There is a clear relationship between  $^{14}\text{C}$  and the nitrogen concentration present in the structural parts of the spent fuel assemblies. The distribution of  $^{14}\text{C}$  in other steel components of the reactor is usually more heterogeneous since it depends on the position of the component relative to the irradiation flux and the thickness of the material. The corrosion rates of stainless and carbon steel are very low in alkaline conditions, even in presence of saline water. The rates are so low that the majority of  $^{14}\text{C}$  is expected to decay in the material. Transition/early phases (oxic phase), or disruptive scenarios with mixed of aggressive species might show higher rates. Recent experimental results from corrosion experiments performed in CAST WP2 indicates release of small organic molecules during anaerobic corrosion of non-activated steel samples. The speciation is dominated by carboxylic acids. Further analysis will determine whether such releases can be expected in disposal conditions. Weak retention of small oxygenated organic compounds in clay and cement environment has been experimentally observed. No compound-specific  $R_d$  values or  $R_d$  values for different classes of organic compounds can be recommended for use in PA due to the limited data set available. Nevertheless, the limited dataset suggests a typical  $R_d$  value of  $10^{-4} \text{ m}^3 \text{ kg}^{-1}$  (upper bound:  $10^{-3} \text{ m}^3 \text{ kg}^{-1}$ , lower bound:  $10^{-5} \text{ m}^3 \text{ kg}^{-1}$ ) for use in PA calculations for all small organic molecules.

The corrosion rate of Zircaloy is very low in alkaline conditions. Similarly, to steel, the majority of  $^{14}\text{C}$  present in Zircaloy will decay in the material before being released. However there remains uncertainties over this release process: Embrittlement of the material is possible due to temperature variations during the interim storage resulting in an orientation change of the hydrides. The additional formation of hydrides in disposal conditions due to the hydrogen pick-up in Zircaloy might affect the surface area exposed to corrosion, especially when the hydrides are oriented in the radial direction. Moreover, the possibility of corrosion regime changes as seen in operational conditions is not excluded. Traditionally, an IRF of 10 to 20% is considered for  $^{14}\text{C}$  in safety assessment. Experimental works in CAST show a very low release of  $^{14}\text{C}$  from the oxide layer. Further analysis is required to clarify whether these measurements are representative of an instant release fraction fit for safety assessment. The hypothesis of a congruent release of  $^{14}\text{C}$  with the corrosion of Zircaloy cannot be confirmed yet.

The representativeness of the samples is particularly challenging in the case of spent ion exchange resins (SIERs). Operational and storage conditions as well as conditioning processes influence the  $^{14}\text{C}$  content in the final waste form. Literature review shows that the organic content of the SIERs vary in a large range in function of the type of reactor. First results in CAST from two leaching experiments from EDF resins (PWR) give reproducible results with 77 % of the total  $^{14}\text{C}$  is under mineral form and the complement on organic form (23%).

$^{14}\text{C}$  is leached from irradiated graphite in organic forms as well as inorganic ( $^{14}\text{CO}_2$ /carbonate) forms. Only a small proportion (a few %) of the  $^{14}\text{C}$  inventory is released in laboratory experiments under alkaline conditions. The proportion of inorganic compounds reported in different sources vary from 20% to 65–75%. Gas phase releases include both volatile  $^{14}\text{C}$ -hydrocarbon/organics (probably  $^{14}\text{CH}_4$ ) and  $^{14}\text{CO}$  but is a small proportion of the total  $^{14}\text{C}$  released. The ratio of  $^{14}\text{C}$ -hydrocarbon/organic compounds to  $^{14}\text{CO}$  in gas for a UK graphite under anaerobic conditions was close to 2:1. The released from irradiated graphite  $^{14}\text{C}$  compounds and ratio between organic/inorganic fraction are under investigation in CAST and these experiments should provide better substantiation of assumptions for safety assessments.

Due to its relatively short half-life, the  $^{14}\text{C}$  radiological flux is sensitive to parameterization of release and migration processes through the disposal system. As inorganic,  $^{14}\text{C}$  is efficiently retarded in clay and cement and its impact is low in the different disposal systems. The retention capacities for the  $^{14}\text{C}$  bearing organics are uncertain. However, due to its relatively short half-life, even a low retention could have discernable effects. The modeling of the retention of  $^{14}\text{C}$  organics will depend on the degree of knowledge on  $^{14}\text{C}$  speciation (e.g. speciation, limited to functional chemical groups), the characteristic of the material (e.g. degradation state of the cement, clay characteristics). The  $^{14}\text{C}$  radiological flux out of the disposal system is sensitive to the instant release fraction for nearly all concepts considered. The  $^{14}\text{C}$  radiological impact might be more pronounced in crystalline rocks because of the shorter transport time through the host rock than in clay and salt systems. The  $^{14}\text{C}$  issue in clay is essentially investigated in gas-phase scenarios where hydrogen is a radionuclide car-

rier. The source term of the exchange ions resins is determined by the cement degradation in safety assessment studies. A good knowledge of the cement evolution is thus important.

## List of Contents

Executive Summary	i
List of Contents	1
List of Figures	2
1 Introduction	3
2 $^{14}\text{C}$ Inventory and Source Terms from different waste materials	4
2.1 Steels (WP2)	4
2.2 Zircaloy (WP3)	6
2.2.1 Zircaloy in the spent fuel assembly	6
2.2.1 Reprocessing waste	15
2.3 Spent ion exchange resins (WP4)	17
2.4 Graphite (WP5)	19
3 Safety Assessment in Clay Disposal Systems	22
3.1 Safety Concept	22
3.2 Scenario analysis	22
4 Safety Assessment in Crystalline Disposal Systems	27
4.1 Safety Concept	27
4.2 Scenario Analysis	27
5 Safety Assessment in Salt Disposal Systems	30
5.1 Safety Concept	30
5.2 Scenario Analysis	30
6 Conclusions	33
References	35
Appendix 1	40
Appendix 2	42
Appendix 3	44
Retention of low molecular weight organics in a cementitious environment (E. Wieland, PSI)	45
Fate of $^{14}\text{C}$ -bearing compounds in clay (Y. Chen <sup>12</sup> , M. A. Glaus <sup>1</sup> , L. R. Van Loon <sup>1</sup> , U. K. Mäder <sup>2</sup> )	47
Chemical interactions of $^{14}\text{C}$ -bearing compounds in salt conditions (B. Kienzler, INE/KIT)	49
$^{14}\text{C}$ investigations in the scope of FIRST-Nuclides (B. Kienzler, INE/KIT)	51
BIOPROTA (Russel Walke, Quintessa)	53

## List of Figures

Figure 1: $^{14}\text{C}$ activity in the steel from different components of light water reactors (LWR).	6
Figure 2: $^{14}\text{C}$ production routes in a LWR assembly.	7
Figure 3: Relative contribution of oxide fuel to total $^{14}\text{C}$ generation in rod in relation to N impurity in fuel and in the Zircaloy. Data from assembly calculations (✖) come from VAN KONYNENBURG [1992], SAKURAGI ET AL. [2013], BORDIER [2008] and ONDRAF/NIRAS, ENRESA and NAGRA in KENDALL ET AL. [2015]. Orange and green lines represent calculated values using ORIGEN2/MCBEND assuming 80 ppm and 40 ppm N in the Zircaloy, respectively.	8
Figure 4: Dependency of $^{14}\text{C}$ activity in oxide fuel (upper) and Zircaloy (lower) on burnup (list of references is given in Appendix 2) and for different levels of nitrogen in the material.	11
Figure 5: Zircaloy-4 claddings – Variations of the axial thickness of zirconia outer layer as a function of the number of cycles [DEHAUDT ET AL., 2000; GRAS, 2014].	12
Figure 6: Variability of the cladding outer oxide layer thickness with Zircaloy cladding types [GEBHARDT AND GOLL, 2012].	12
Figure 7: Temperature evolution of the spent fuel from interim storage to final disposal [BOULANGER ET AL., 2005].	15
Figure 8: Waste processing streams. Solid and dash arrows refer to different hypotheses regarding the carry over fraction of $^{14}\text{C}$ upon spent fuel assemblies reprocessing.	16
Figure 9: $^{14}\text{C}$ production in LWR coolant and typical release fractions [EPRI, 2010; IAEA, 2004; SKB, 2005].	17
Figure 10: Dose curve calculated for an HLW repository in the siting Zurich Northeast, alternative Case ‘Unfavourable Diffusion Coefficients’ [NAGRA, 2014e, 2014d]. Ch-14 = organic $^{14}\text{C}$ IRF, Ch- $^{14}\text{C}$ = organic $^{14}\text{C}$ CR.	24
Figure 11: Evolution of $^{14}\text{C}$ concentrations in the near field of a repository as calculated by the CIGEO project [KAEMPFER AND SCHAEDELE, 2016].	26
Figure 12: Mass balance of $^{14}\text{C}$ as calculated by the CIGEO project [KAEMPFER AND SCHAEDELE, 2016].	27
Figure 13: Transport paths in crystalline host rock [JAEA AND FEPC, 2007].	29
Figure 14: Expected dose rate for the base case scenario of the Loviisa repository with conservative parameter values [EURAJOKI, 2008; EURAJOKI, 2006].	29
Figure 15: Contribution of different waste materials to the overall dose rate as calculated by JAEA AND FEPC [2007] and SAKURAGI ET AL. [2013].	30
Figure 16: Performance indicator (RGI) resulting from the $^{14}\text{C}$ flux out of the spent fuel containers calculated (dimensionless unit) [LARUE ET AL., 2013].	32

## 1 Introduction

Work Package 6 (WP6) of the CAST project assists organisations in charge of the long-term management of radioactive waste (mainly Waste Management Organisations, WMOs) to implement the results produced in WP2 to WP5 at the scale of their repository system and to analyse the impact of these results on long-term safety. WP6 can be seen as an integration exercise to ensure that the results from WP2 to WP5 are relevant to the safety cases for the CAST end-users, the WMOs.

Prior to the analysis of the experimental results delivered by the project, the first phase of WP6 aims at taking stock of the  $^{14}\text{C}$  treatment in recent safety assessments. CAST deliverable D6.1 [KENDALL ET AL., 2015] gives an overview on this from the national programs' perspective. Deliverables D2.1, D3.1, D4.1 and D.5.5 provide a state-of-the-art of  $^{14}\text{C}$  speciation and release in steel, Zircaloy, ion exchange resins and graphite, respectively. On the basis of these reviews, commonalities and differences between disposal concepts regarding  $^{14}\text{C}$  fate have been identified. In addition, conservatisms used in safety assessment to cope with the uncertainties were discussed. The following topics are addressed in this deliverable D6.2 and structured according to (i)  $^{14}\text{C}$  inventories and source terms of the four waste materials investigated in CAST (ii)  $^{14}\text{C}$  transport in different host rock formations.

## 2 $^{14}\text{C}$ Inventory and Source Terms from different waste materials

The synopsis of  $^{14}\text{C}$  inventories has two objectives: (i) it allows for a consistency check of the inventories, and (ii) it provides a comparison between measured and calculated activities of  $^{14}\text{C}$ .

$^{14}\text{C}$  release from a spent fuel assembly as calculated in safety assessment originates not only from the claddings but also from the UOx fuel and the structural parts. In the case of the reprocessing waste like the compacted waste, the hypothesis regarding the  $^{14}\text{C}$  source term depend on the inventory in the different parts of the assembly, including the UOx matrix. For this reason, it was valuable in WP6 to review the hypothesis on  $^{14}\text{C}$  in the fuel matrix although it is not strictly speaking part of CAST. The rest of this section is structured according to the materials studied in CAST. The part covering  $^{14}\text{C}$  inventory in Zircaloy includes a discussion of  $^{14}\text{C}$  in the spent fuel matrix and in reprocessing waste. The  $^{14}\text{C}$  inventory table for different waste types derived from KENDALL ET AL. [2015] is given in Appendix 1.

### 2.1 Steels (WP2)

Figure 1 shows the  $^{14}\text{C}$  activity in steel from different components of light water reactors (LWR) as provided by WP6 contributors. The correlation of  $^{14}\text{C}$  with the nitrogen content is very well reproduced for the structural parts. However, there is no clear correlation for core internals and pressure vessels, most likely due to the employed calculation methodology/assumptions. Based on past studies indicating experimental evidences of carbon released as volatile short chained aliphatic hydrocarbons species [SWANTON ET AL., 2015], safety assessments usually considers  $^{14}\text{C}$  as 100% soluble organic and/or gaseous hydrocarbons, usually methane [KENDALL ET AL., 2015]. Recent experimental results from corrosion experiments performed in CAST WP2 indicates release of small organic molecules during anaerobic corrosion of non-activated steel samples. The speciation is dominated by carboxylic acids. The contribution from volatile compounds (aldehydes and alkanes) is minor. The concentration decreases with increasing carbon chain length. There are indications that these organic releases originate from the oxidation layer. These preliminary results have to be

confirmed with activated samples in CAST [MIBUS ET AL., 2015; see also abstracts of WIELAND and of CHEN ET AL. in APPENDIX 3]. Implications on safety assessment will be discussed in future steps of CAST.

In the framework of the CAST project, a comprehensive review of steel corrosion rates has been carried out [SWANTON ET AL., 2015]. Corrosion rates in alkaline conditions are very low because of the passive protective film. The passivation layer develops within few hours to tens of days, limiting greatly the short-term active corrosion.

Many experimental studies have shown that uniform corrosion rates for carbon steel in anoxic, alkaline conditions are below  $0.1 \mu\text{m}/\text{yr}$ . Recently, an increasing number of studies indicate upper values in the range of few tens of  $\text{nm}/\text{yr}$  [NAGRA, 2014a; SMART ET AL., 2014]. Corrosion studies in unsaturated conditions have shown even lower rates [NAGRA, 2016]. There is little effect of  $\gamma$ -irradiation, chloride or sulphur species and temperature on long-term anoxic corrosion due to the mentioned passivation [SWANTON ET AL., 2015]. Corrosion rates can be higher during transient periods, when oxidic conditions prevail and aggressive species are present [ONDRAF/NIRAS, 2008].

Uniform corrosion rates for stainless steel are very low. In anoxic, alkaline conditions, recent measurements report values below  $0.01 \mu\text{m}/\text{yr}$  [SWANTON ET AL., 2015]. Chloride is unlikely to affect the corrosion rate in anoxic conditions. Recently, SAKURAGI ET AL. [2016] have measured corrosion rates of  $0.4 \text{ nm}/\text{yr}$  over 6 years.

The corrosion rates of stainless and mild steels are higher in neutral conditions than in alkaline conditions. This might affect the  $^{14}\text{C}$  release in pessimistic scenario where the alkalinity of the near field decreases i.e., because of ageing of the cementitious environment (see Figure 14 and associated discussion in Section 4.2). However, the impact remains limited since the pH decreases significantly only in the long-term (after phase 1 and 2 of the cementitious evolution) when much of the  $^{14}\text{C}$  has decayed.

Usually no instant release fraction is considered for steel in safety assessment. The passivation layer is so dense that a rapid and substantial release is not expected.

[NAGRA, 2014b] assume an instant release fraction (IRF) in mixed metallic wastes. In or-

der to accommodate the heterogeneous  $^{14}\text{C}$  distribution in large steel pieces like reactor internals, the  $^{14}\text{C}$  activity is function of the thickness or supposed to be mainly located in small pieces or near the material surface giving rise to an overestimated radiotoxic peak in safety assessments [KENDALL ET AL., 2015].

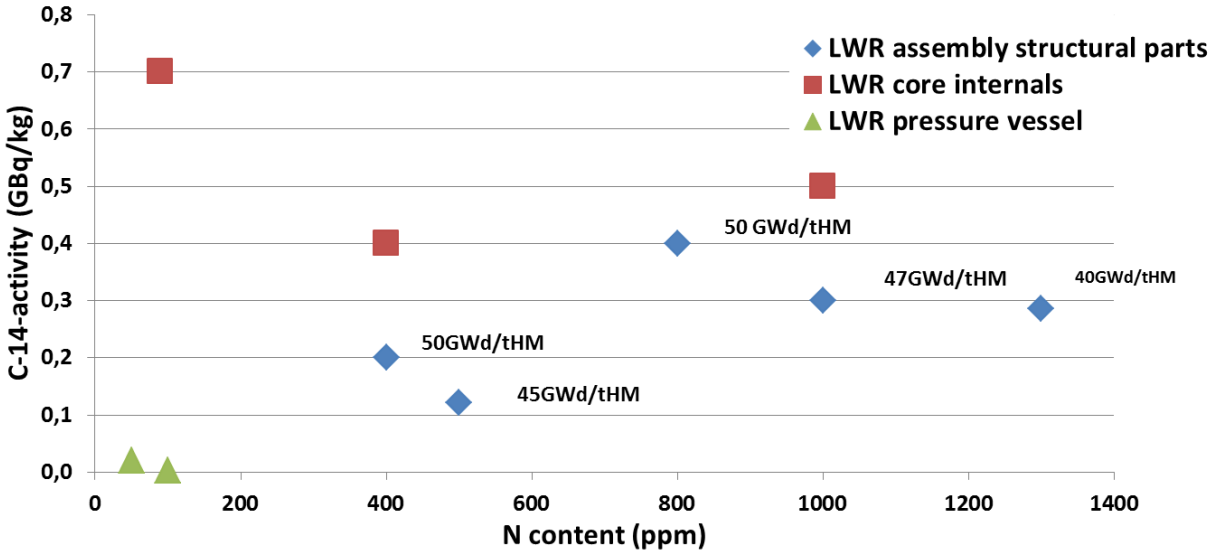


**Figure 1:  $^{14}\text{C}$  activity in the steel from different components of light water reactors (LWR).**

## 2.2 Zircaloy (WP3)

Zircaloy is a material found in two distinct classes of waste: as constituent of the claddings of a fuel assembly on the one hand, and as major component of the reprocessing waste on the other hand (the compacted waste, CSD-C).

### 2.2.1 Zircaloy in the spent fuel assembly

The activity and distribution of  $^{14}\text{C}$  within the three constituents of a fuel assembly (fuel, cladding, structural parts) depends on, (i) the concentration of N impurity in the components, (ii) the fuel's initial enrichment, (iii) the fuel burn-up, and (iv) the assembly irradiation conditions.

Figure 2 illustrates the two major routes of  $^{14}\text{C}$  production for a light water reactor (LWR) fuel assembly. The relative contribution of the different routes in the fuel assembly (mainly from  $^{14}\text{N}$  and  $^{17}\text{O}$  activation) depends notably on the N impurity assumed for each of the source components. The Zr cladding may include a non-negligible contribution from the oxygen of the water coolant (conversion of  $^{17}\text{O}$  incorporated through the corrosion process). Depending on these assumptions, the contribution of the oxide fuel to the overall  $^{14}\text{C}$  production in the fuel assembly varies typically between 30% and 90%.

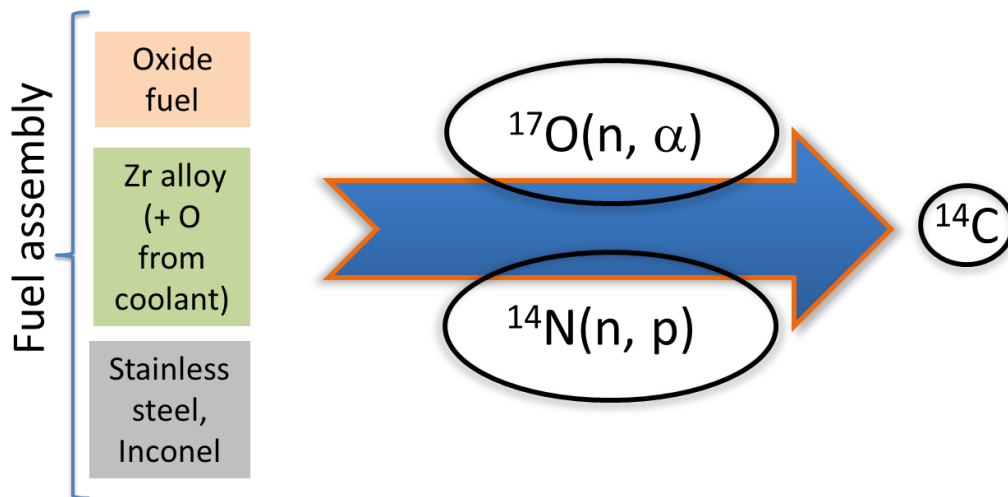


**Figure 2:  $^{14}\text{C}$  production routes in a LWR assembly.**

Figure 3 illustrates the importance of the N impurity in the fuel on the relative contribution to the overall  $^{14}\text{C}$  generation in the fuel rods. The orange and green lines represent calculated values<sup>1</sup> of the oxide fuel contribution for assumed N impurities of 80 ppm and 40 ppm in the Zircaloy cladding. With larger N impurities in the fuel, the contribution of the oxide fuel to the overall  $^{14}\text{C}$  production increases from 35 - 50% to 80 - 90%. The considered values

<sup>1</sup> For the fuel and for the cladding part along the active length,  $^{14}\text{C}$  mass inventories were calculated with ORIGEN2 and for the cladding part outside the active length, activation rates were calculated with the Monte Carlo code MCBEND.

for the  $\text{UO}_x$  contribution in safety assessments depend on the level of conservatism of the assumed N-content in the Zircaloy. While an N content of 40 ppm can be seen as a more realistic value, a conservative value of 80 ppm, is often considered in safety assessments due to specification of manufacturers. Figure 3 shows that the values for the oxide fuel contributions provided in CAST and in the literature are consistent if the assumed N impurity of the Zircaloy is taken into account.

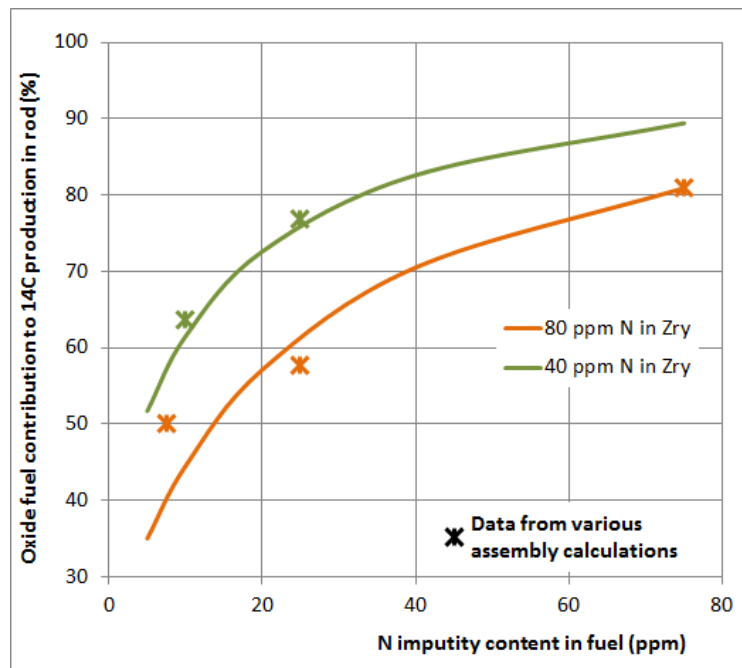


**Figure 3: Relative contribution of oxide fuel to total  $^{14}\text{C}$  generation in rod in relation to N impurity in fuel and in the Zircaloy. Data from assembly calculations ( $\times$ ) come from VAN KONYNENBURG [1992], SAKURAGI ET AL. [2013], BORDIER [2008] and ON-DRAF/NIRAS, ENRESA and NAGRA in KENDALL ET AL. [2015]. Orange and green lines represent calculated values using ORIGEN2/MCBEND assuming 80 ppm and 40 ppm N in the Zircaloy, respectively.**

Figure 4 shows the general increase of  $^{14}\text{C}$  activities with burn-up in the oxide fuel (upper) and in the Zircaloy material of the spent fuel assembly (lower) based on measured and calculated data. Concerning the calculated data, one notes a general good agreement between the different codes/methodologies used, for a given nitrogen initial content.

As regards the  $^{14}\text{C}$  content in fuel, the trend line for the measured data is representative of an initial nitrogen content of 20-30 ppm (as based on the calculations). The maximum measured  $^{14}\text{C}$  inventory does not exceed the calculated values using 75 ppm initial nitrogen

content. Setting  $N=75$  ppm in calculations for safety assessments for UOx seems *a priori* fully conservative.

As regards the  $^{14}\text{C}$  content in the cladding, most of the experimental data are representative of an initial nitrogen content of 30-40 ppm. Note that the experimental data set includes measurements on cladding material sampled from an assembly operated in high thermal conditions (i.e. not representative of a standard operation). For most of these samples, the as-measured inventory exceeds  $^{14}\text{C}$  contents as calculated with 80 ppm nitrogen initial content. This seems to indicate that for a (very) limited amount of spent assemblies, an additional (coolant) contribution to the  $^{14}\text{C}$  inventory should be expected. Setting  $N=80$  ppm in calculations for safety assessments for Zircaloy seems however reasonably conservative.

The distribution of the  $^{14}\text{C}$  activities among the different waste materials has important implications for the derivation of the source term for safety assessment.  $^{14}\text{C}$  release is specified either as an instant release fraction (IRF) or as congruent release (CR). For oxide fuel a conservative IRF of 10% is usually used in performance assessment [KENDALL ET AL., 2015]. This fraction is based on the review of leaching measurements from CANDU and LWR fuels made by JOHNSON AND TAIT [1997]. The data are scarce but indicate IRFs  $< 5\%$  for low temperature. More recently, [JOHNSON ET AL., 2005; NAGRA, 2014c] confirmed the conservative value of 10% for performance assessment. FERRY et al. [2008] notes that the diffusion processes of  $^{14}\text{C}$  and  $^{36}\text{Cl}$  in the UOx matrix remain an open question. ANDRA [2005] considers a contribution from alpha-self-irradiation enhanced diffusion for these two nuclides in their IRF. In the framework of the *FIRST-Nuclides* project, an instant release fraction of  $^{14}\text{C}$  of 1% to 2% was determined in leaching experiments (see abstract of KIENZLER in APPENDIX 3). The speciation of  $^{14}\text{C}$  in spent fuel UOX is uncertain but because of the long containment times and/or the stability of the matrix, decay of  $^{14}\text{C}$  occurs before its actual release to the geological environment.

The oxide thickness at the surface of the Zircaloy claddings depends on many factors such as burn-up, operating conditions and cladding types. Figures 5 and 6 illustrate the evolution of the zirconia outer layer thickness with the number of burn-up cycles. The oxidation profile is related to the temperature gradient of the water coolant. Figure 6 shows the variability

of the zirconia outer layer thickness for different cladding types and burn-up. Maximum values of 100  $\mu\text{m}$  are only observed locally in the upper part of a Zy-4 cladding in the PWR conditions. This limit provides a basis to derive a conservative estimate of the IRF in safety assessments. According to [GEBHARDT AND GOLL, 2012], the typical corrosion layer thickness of BWR fuel rods remain below 100  $\mu\text{m}$  up to high burnups.

Measurements on LWR hulls indicated that the  $^{14}\text{C}$  concentration in the oxide layer is roughly two to four times its concentration in the bulk metal [GRAS, 2014; GUENTHER ET AL., 1990].  $^{14}\text{C}$  production from the  $^{17}\text{O}(n,\alpha)^{14}\text{C}$  reaction could justify this inventory increase into the oxide layer, but only partially. Another hypothesis put forward by YAMAGUCHI [1999] was a mechanism in which  $^{14}\text{C}$  is not released immediately by corrosion but is incorporated into the zirconium oxide film. This kinetic could not be confirmed yet.

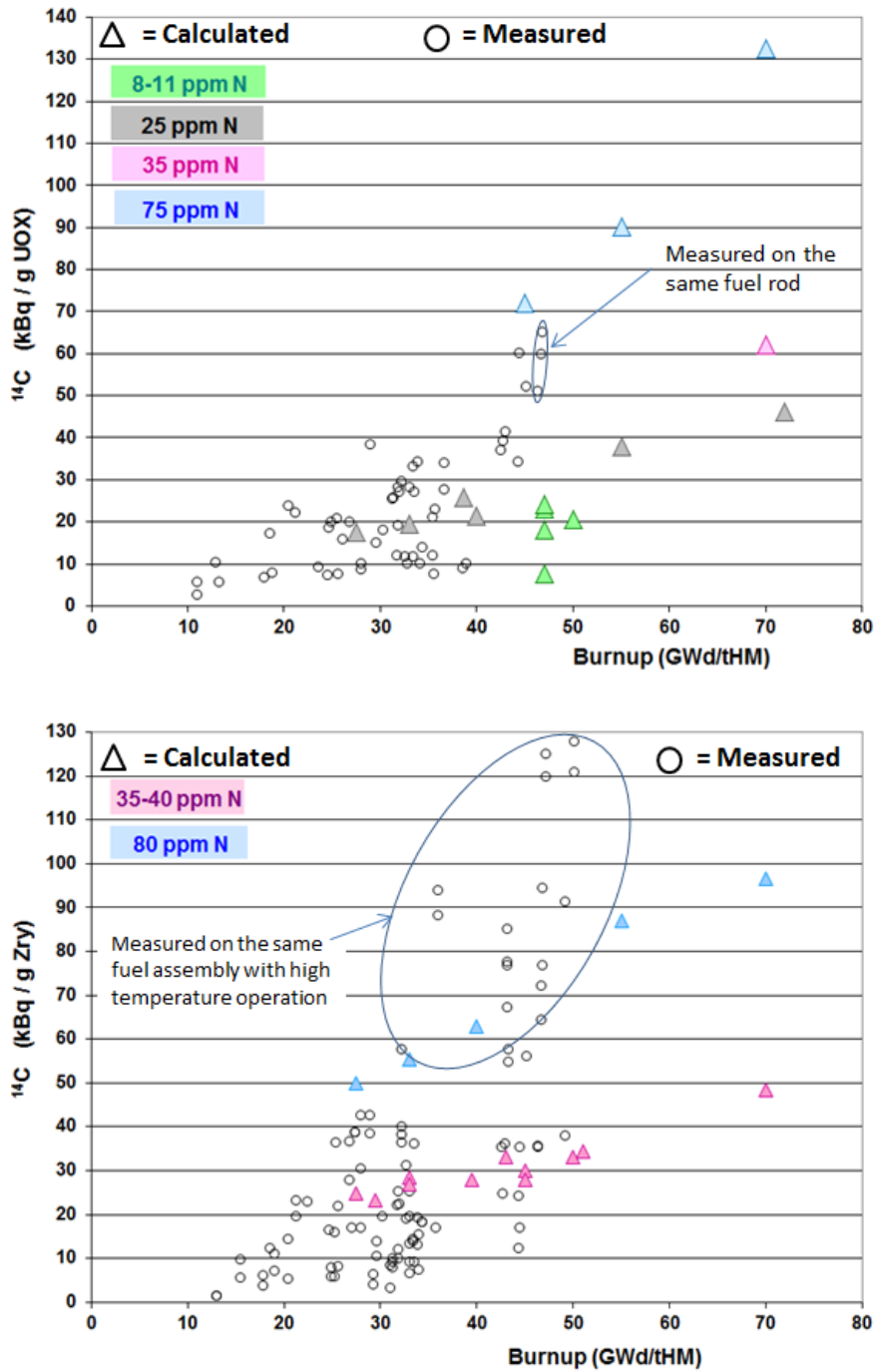


Figure 4: Dependency of  $^{14}\text{C}$  activity in oxide fuel (upper) and Zircaloy (lower) on burnup (list of references is given in Appendix 2) and for different levels of nitrogen in the material.

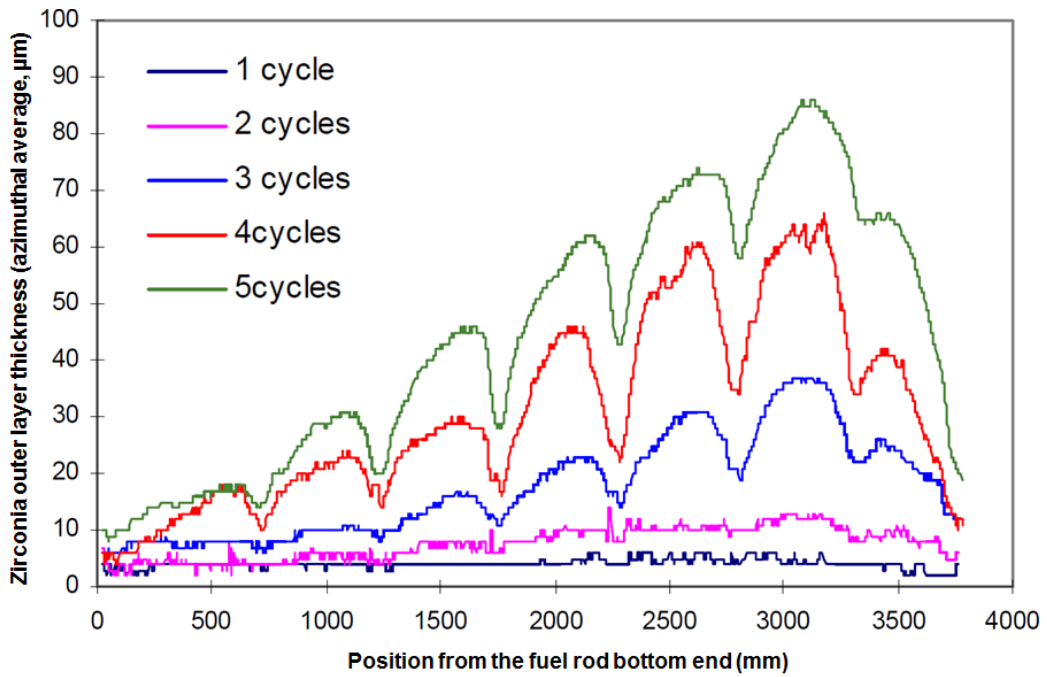


Figure 5: Zircaloy-4 claddings – Variations of the axial thickness of zirconia outer layer as a function of the number of cycles [DEHAUDT ET AL., 2000; GRAS, 2014].

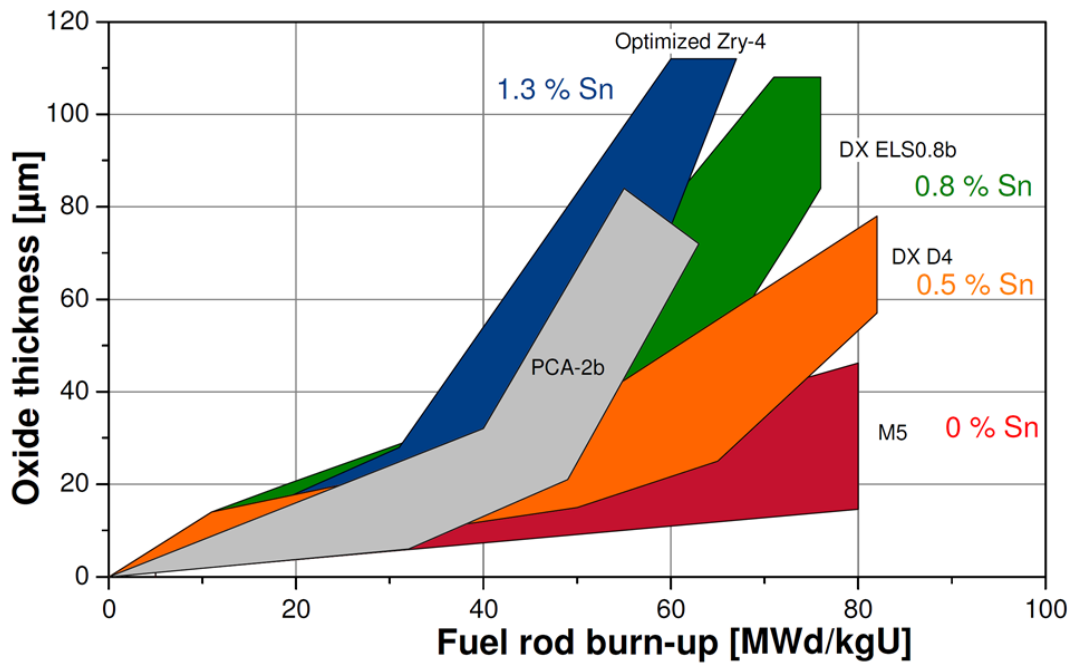


Figure 6: Variability of the cladding outer oxide layer thickness with Zircaloy cladding types [GEBHARDT AND GOLL, 2012].

Leaching tests of PWR & BWR hulls in alkaline solutions (sea water derived groundwater equilibrated with cement) and room temperature were carried out by RWMC. The observations indicate a very low  $^{14}\text{C}$  release fraction (lower than 1 %) after two years from both hulls with and without oxide layers [references in GRAS, 2014]. These results do not suggest the existence of an instantaneous  $^{14}\text{C}$  release of hulls in these conditions. The possible abstraction of these experimental results (e.g. characteristic of the zirconia, impact of experimental conditions) in sound release parameters for assessment in geological conditions will be the object of further discussions in CAST. The IRFs for  $^{14}\text{C}$  considered traditionally in safety assessment are much higher, as for example, an IRF of 10 to 20% for Zircaloy-4 claddings. It may be possible to employ less conservative values when specific cladding types are considered [KENDALL ET AL., 2015]. Indeed, the thickness of the oxide layer is lower for M5 (less than 40  $\mu\text{m}$ ) as well as for ZIRLO<sup>2</sup> (less than 70  $\mu\text{m}$ ). Note that the inner side of the cladding in contact with uranium dioxide develops also an oxide layer in operational conditions (maximum thickness around 10  $\mu\text{m}$ ). Its conceptualisation in safety assessment is rarely reported but its treatment seems to be similar to (and taken together with) the external layer. [GRAS, 2014] made an extensive review on the  $^{14}\text{C}$  release from Zircaloy under repository conditions. The corrosion regime of Zircaloy in high temperature water changes when the zirconia layer reaches a critical thickness of 2.5  $\mu\text{m}$ . At this point, there is a destabilization of the oxide layer, as a result of which, the passivating layer becomes porous and fractured due to the relaxation of internal stresses [ALLEN ET AL., 2012]. The kinetic law switches to a pseudo-linear regime, which is constituted by the cyclic succession of several cubic regimes, accelerating the corrosion rate. It is difficult to make assumptions on the occurrence of this phenomenon in disposal environments where the chemical and thermal conditions are significantly different. In addition, hydrides are formed in the bulk of the claddings during operation in the reactor. Cooling processes during transport and interim storage induce precipitation and reorientation of the hydrides resulting in an embrittlement of the cladding, which in turn might increase the surface area exposed to corrosion, especially when the cracks are oriented in the radial direction [CHU ET AL., 2008]. This effect might increase radionuclide release in disposal conditions. The hydrogen pick-up ratio of

---

<sup>2</sup> ZIRLO is a Westinghouse design and M5 is an AREVA design

Zircaloy-4 is about 90% in alkaline and neutral conditions between 30 and 50°C. It follows that the production of hydrogen in disposal conditions might not be congruent with the corrosion of the metal. The hydrogen pick-up ratio is considerably less for claddings less prone to oxidation like M5 types.

The contribution of crud (surface deposits) from the primary coolant to the <sup>14</sup>C inventory has been considered by SKB [2010]. No value was reported for <sup>14</sup>C. However, crud contribution to radionuclide inventory of canister is estimated to be several orders of magnitude lower than the total inventory.

The review made by [GRAS, 2014] indicates corrosion rates for Zircaloy (at low temperature, in alkaline or neutral conditions, after a few years) of the order of few nm/y at the most. This review is in line with [SHOESMITH AND ZAGIDULIN, 2011], who suggest that corrosion rates of a Zircaloy spent fuel cladding should not be higher than 5 nm/y. Preliminary results gathered in the CAST project [JOBAGY ET AL., 2015] of oxidised Zr-4 in deaerated conditions and in alkaline conditions is in agreement with these values with corrosion rates of a few nm/year, at most, after several years. Rates in aerated conditions are several times higher. Consequently, the rates used in safety assessments range from a few nm/y to 10 nm/y and are thus appropriately conservative [ANDRA, 2005; NAGRA, 2014c].

Pitting corrosion is not expected in neutral and alkaline anoxic conditions, independent of the cladding surface conditions and even at chloride concentrations close to seawater. However, pitting corrosion cannot be excluded in high chloride and oxic conditions (transitional regime) [GRAS, 2014].

Higher temperature increases the solubility of zirconia. The speciation of <sup>14</sup>C released from the claddings is uncertain. Different hypotheses of speciation have been thus tested in safety assessments. The Japanese experimental program reviewed by [GRAS, 2014] indicates the presence of organic compounds. Preliminary CAST results report the predominance of organic species in both, the aqueous and the gaseous phase [JOBAGY ET AL., 2015]. The hypothesis of a congruent release could not be confirmed yet possibly because the radionuclides are incorporated in the oxide film. Thermal diffusion of <sup>14</sup>C during transportation and dry storage can be significant due to the high temperatures (Figure 7) [GRAS, 2014 and ref-

erences therein]. The release in an inert atmosphere may be less sensitive to temperature compared to the release in air. Under repository or dry storage conditions, thermal out-diffusion of  $^{14}\text{C}$  cannot be excluded and could affect the initial  $^{14}\text{C}$  inventory located in the top layers of 100  $\mu\text{m}$  thickness.

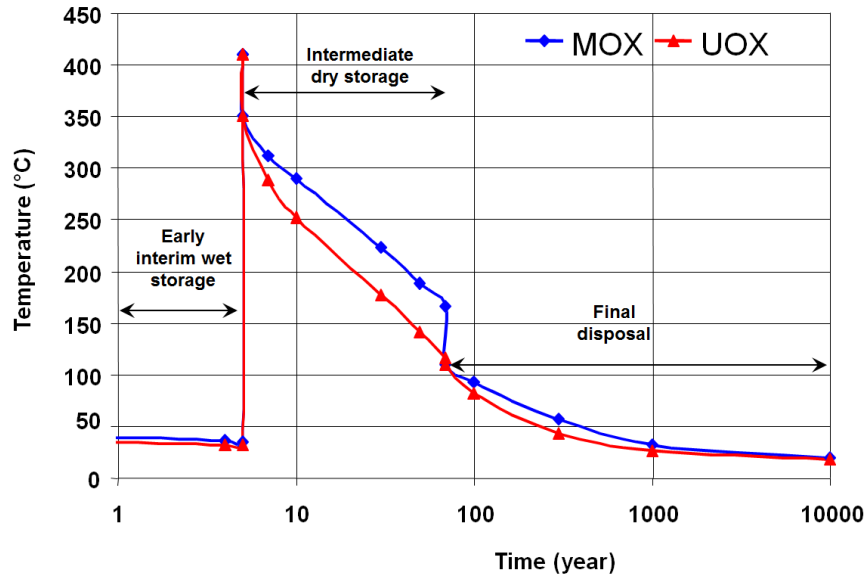


**Figure 7: Temperature evolution of the spent fuel from interim storage to final disposal [BOULANGER ET AL., 2005].**

### 2.2.1 Reprocessing waste

The reprocessing of spent nuclear fuel assemblies by AREVA generates high-level glass waste (CSD-V) and compacted waste (CSD-C). The determination of the  $^{14}\text{C}$  inventory in these two types of waste is based on assumptions on the carry over fractions from the different components of the assemblies [CARUSO ET AL., 2015; CROZET ET AL., 2016]. The  $^{14}\text{C}$  inventory in the CSD-V might originate both from residuals of the cut cladding and assembly structures in the dissolution solution or from the oxide fuel. CROZET ET AL. [2016] has provided an experimental evaluation of the  $^{14}\text{C}$  inventory from the fuel assembly that is present in the unfiltered dissolution solution but various assumptions are still made regarding the fraction of  $^{14}\text{C}$  from oxide fuel inventory that effectively ends up in the CSD-V. BARTAGNON [2003] give a conservative limit of 10% for this fraction (Figure 8).

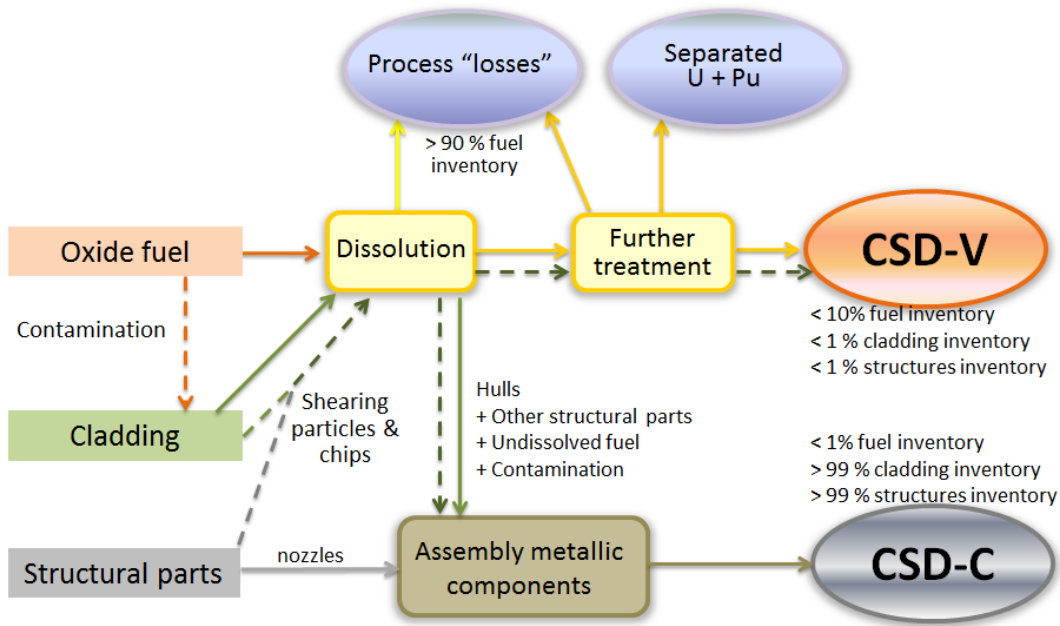


**Figure 8: Waste processing streams. Solid and dash arrows refer to different hypotheses regarding the carry over fraction of <sup>14</sup>C upon spent fuel assemblies reprocessing.**

Because of this uncertainty on the fuel contribution, the <sup>14</sup>C inventory in vitrified waste can vary by one order of magnitude and reach 10 GBq by canister. Large uncertainties also exist concerning the speciation of <sup>14</sup>C in reprocessing waste and the dominant forms of <sup>14</sup>C release in disposal conditions (organic versus inorganic).

In addition to the inventory for the claddings and the structural parts, the <sup>14</sup>C inventory in CSD-C might include a minor contribution from the oxide fuel. The <sup>14</sup>C inventory of compacted waste with a nitrogen concentration of 80 ppm is between 15 and 45 GBq per primary package for average burn-ups between 33 and 45 GWd/tHM. The incorporation of the reprocessing waste has evolved towards higher incorporated volumes and ranges between 0.5 and 0.8 CSD-V or CSD-V/tHM depending on the campaign.

Accounting for an instant release fraction from compacted waste is still a matter of debate. In theory, the IRF used for the cladding of directly disposed spent fuel should also be applicable to CSD-C. The compaction process is not expected to reduce the specific surface area. However, the acid treatment of the material during reprocessing might remove accessible <sup>14</sup>C from the surfaces [KENDALL ET AL., 2015]. Consequently, the IRF for CSD-C may range

from 0% to 20%, without counting the potential IRF associated to shearing and dissolution fines included in the waste form.

**2.3 Spent ion exchange resins (WP4)**

The activity of <sup>14</sup>C in spent ion exchange resin (SIER) as considered by the different participants of the CAST project ranges from 0.1 to 10 MBq/kg [KENDALL ET AL., 2015]. The state-of-the art review by [RIZZATO ET AL., 2015] indicates that the range of activity depends on several specific factors such as reactor type, resin type as well as storage, handling and conditioning of the resin. Therefore, the source terms are based on different assumptions that are specific for the respective operation conditions. Most resins discussed here originate from the reactor coolant (condensate clean up resins and reactor coolant clean up resins).

In boiling water reactors (BWRs), oxidizing conditions typically lead to the formation of more oxidized species, i.e., end-product CO<sub>2</sub> and carbonate. Pressurized water reactors (PWRs), on the other hand, produce mainly reduced species, i.e., end-product CH<sub>4</sub>. EPRI [2010], SKB [2005] and IAEA [2004] have evaluated the organic fraction contained in the exchange resins. This information is synthesized in Figure 9.

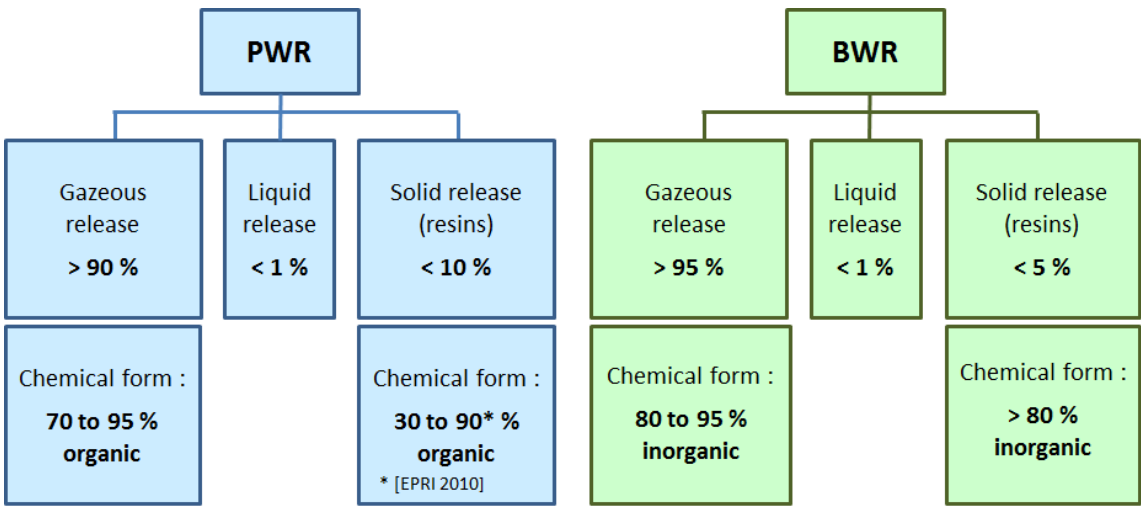


**Figure 9: <sup>14</sup>C production in LWR coolant and typical release fractions [EPRI, 2010; IAEA, 2004; SKB, 2005].**

Typical fractions of organics in PWR coolant represent more than 60% whereas for BWR the organic fraction is minor. Equal proportions of organic and inorganic <sup>14</sup>C species have been

found in two SIER samples from RMBK graphite-moderated boiling reactors. For CANDU PWRs 5% to 20% organics have been measured [references in RIZZATO ET AL., 2015]. However, data are scarce and not comparable. First results in CAST from leaching experiments from EDF resins (PWR) indicate that about 20% of  $^{14}\text{C}$  are in organic form [BUCUR ET AL., 2015].

REILLER ET AL. [2014] report that storage and conditioning influences significantly the  $^{14}\text{C}$  content in the final waste form (e.g. activities between dried and wet resins, impact of a mixed bed, temperature influence). As an example, SKB observed that air bubbling used as a stirring method leads to a loss of inorganic  $^{14}\text{C}$  activity. However, these losses are difficult to quantify.

$^{14}\text{C}$  release from IERs in safety assessment is assumed to be governed by the degradation of the concrete packages. The assumed organic fraction is variable and depends on the operation conditions, the reactor type and the processing of the spent resins [KENDALL ET AL., 2015]. Additional measurements of the fraction of organic  $^{14}\text{C}$  in SIERS as a function of these parameters would improve the knowledge associated to the release behaviour.

## 2.4 Graphite (WP5)

The main source of  $^{14}\text{C}$  generation in graphite is the result of the following reactions:  $^{14}\text{N}(n,p)^{14}\text{C}$ ,  $^{13}\text{C}(n,\gamma)^{14}\text{C}$  and  $^{17}\text{O}(n,\alpha)^{14}\text{C}$  [IAEA, 2006]. The largest amount of irradiated graphite (i-graphite) comes from the reactors where graphite is used as moderator and reflector (e.g. Magnox, RBMK). However, there are also other sources of i-graphite, e.g. thermal column of research reactors. The activity of  $^{14}\text{C}$  in the i-graphite depends on the location in the reactor core, operating power history, initial concentration of impurities, amount of cooling gases, etc. Specific activity of  $^{14}\text{C}$  in i-graphite as considered by the participants of the CAST project varies in a wide interval from  $1\text{E-}5$  GBq/kg to 1 GBq/kg [CATHERIN ET AL., 2016; KENDALL ET AL., 2015]. This variation reflects not only the differences in the origin and the irradiation history of graphite but also the differences in the assumptions when deriving the inventory. The method used to assess the  $^{14}\text{C}$  inventory by ANDRA was based on computation and radiochemical measurements. LEI estimated the inventory using computer tool ORIGEN-S for a very conservative case. The assumptions were the following: a maximal thermal neutron flux, a maximal initial nitrogen concentration in the graphite matrix (70 ppm) and the presence of nitrogen from the cooling gases in all (open and closed) graphite pores.  $^{14}\text{C}$  in irradiated graphite from the thermal columns of research reactors in Romania relies on ORIGEN simulations coupled with experimental measurements [KENDALL ET AL., 2015].

The chemical form of  $^{14}\text{C}$  in i-graphite is not well known as well as the mechanisms by which it is released from i-graphite in disposal conditions [KENDALL ET AL., 2015]. Therefore, an empirical approach is used in safety assessment based on the assumption of a release rate proportional to the activity of  $^{14}\text{C}$  in i-graphite.

Experimental results indicate  $^{14}\text{C}$  release at an initial (high) release rate, which is followed by a decreasing release rate in the long-term [NDA, 2016; TOULHOUT ET AL., 2015]. The rapidly releasable  $^{14}\text{C}$  is associated with  $^{14}\text{C}$  absorbed onto the graphite surfaces and pores while slowly releasable fraction of inventory is attributed to  $^{14}\text{C}$  incorporated in the crystal lattice or at an interstitial position. The most recent leaching experiments performed with

UK graphite revealed that even under harsh acidic conditions, not more than 30% of the  $^{14}\text{C}$  could be released [NDA, 2016]. This provided evidence that not all of the  $^{14}\text{C}$  is releasable.

The review presented in [TOULHOUT ET AL., 2015] indicates that decrease in the total  $^{14}\text{C}$  release rate to solution is observed over a period of 10 to 100 days. The timescale to reach the quasi-steady state leach rate for the French stack graphite appears to be around 100 to 200 days and in the experiments with UK graphite the steady state leaching rate is reached under most conditions after 90 days. The short period for rapid release is also pointed out in AMEC [2016], where it is indicated that the rapid release will occur over such a short time that for long-term modelling it may be better considered as an initial instant release.

It should be noted also that the initial rapid release of  $^{14}\text{C}$  from intact graphite was not seen for crushed graphite [TOULHOUT ET AL., 2015]. Therefore, the labile fraction might be lost during treatment of i-graphite.

Differences in leachability of  $^{14}\text{C}$  from i-graphite are taken into account in safety assessment by defining an appropriate leaching rate for specific fractions of the inventory. In a conservative case of LEI assessment, it is assumed that all  $^{14}\text{C}$  is releasable and only two fractions (rapid release and slow release) are distinguished. The rapid release is modelled by assuming that 10% of the inventory is released per year over a period of 10 years [KENDALL ET AL., 2015]. In a more realistic case (RWM), the fraction of  $^{14}\text{C}$  activity in the graphite that is available for rapid release varies from 0 to 0.002 and the fraction for slower release varies from 0.01 to 0.3. The rest of the inventory is considered as non-releasable [NDA, 2016].

The difference between treated and non-treated i-graphite in the safety assessment is considered by assuming no rapid release for treated graphite.

Results of the leaching experiments show in general a very slow  $^{14}\text{C}$  release rate (usually less than 1% over timescales up to 3 to 4 years) [TOULHOUT ET AL., 2015]. Total fractional releases obtained in laboratory experiments vary by two to three orders of magnitude. This reflects the different sources, irradiation histories and irradiation conditions of the graphite. It is also indicated in [TOULHOUT ET AL., 2015] that the leaching rate depends on the shape

of the sample: with increase in geometric surface area increase in  $^{14}\text{C}$  release to solution is observed.

Studies of leaching of moderator and reflector graphite from the Tokai (Magnox) reactors (Japan) in alkaline solution revealed that about 0.1% of the total  $^{14}\text{C}$  inventory of the graphite samples was released to solution over three years (with the majority of the release occurring in the first month) [TOULHOUT ET AL., 2015]. Experiments with Oldbury graphite samples (UK) under the baseline conditions (anoxic, at pH = 13 solution, ambient temperature) indicated that about 0.07% of the  $^{14}\text{C}$  inventory is released to solution in one year [AMEC, 2014].

Rate constant for the long-term release of  $^{14}\text{C}$  from i-graphite selected in the safety assessment varies from 0.001 to 0.1 1/y [NDA, 2016; KENDALL ET AL., 2015]. However, some bounding cases with instant release and very low release rate (of the order of  $1\text{E}-05$  1/y) are also analysed.

The majority of  $^{14}\text{C}$  release from i-graphite occurs to the solution phase and only small amounts of gaseous phase releases (about 1% of the released  $^{14}\text{C}$ ) have been measured [TOULHOUT ET AL., 2015].

Under alkaline conditions,  $^{14}\text{C}$  is released to the liquid phase in hydrocarbon/organic forms as well as inorganic ( $^{14}\text{CO}_2$ /carbonate) forms. According to some sources reported in [TOULHOUT ET AL., 2015] and information provided in [CATHERIN ET AL., 2016], amount of inorganic compounds in solution can vary between 65–75%. However, the leaching experiments with graphite from the Tokai (Magnox) reactors (Japan) indicated that about 80% of the carbon-14 released was in organic form with only 20% as carbonate [TOULHOUT ET AL., 2015].

Gas phase releases at high pH include both volatile  $^{14}\text{C}$ -hydrocarbon/organics (probably  $^{14}\text{CH}_4$ ) and  $^{14}\text{CO}$  [TOULHOUT ET AL., 2015]. In the gas-phase release at pH 13 and under anaerobic conditions the ratio of  $^{14}\text{C}$ -hydrocarbon/organic compounds to  $^{14}\text{CO}$  was close to 2:1 [AMEC, 2014]. The form of gaseous  $^{14}\text{C}$  release is affected by redox conditions. The

lower redox seems to favour  $^{14}\text{C}$ -hydrocarbon/organic compounds [TOULHOUT ET AL., 2015].

In safety assessment, the release of volatile  $^{14}\text{C}$  is assumed to be 100% in the form of methane. In regard to  $^{14}\text{C}$  in solution (transport by the groundwater pathway) the assumption usually is that all  $^{14}\text{C}$  is present in inorganic form. However, as a conservative case also variant with 100% of organic  $^{14}\text{C}$  in solution might be considered [KENDALL ET AL., 2015].

### 3 Safety Assessment in Clay Disposal Systems

#### 3.1 Safety Concept

The safety concept in a clay disposal system is based on the multi-barrier principle. The disposal system comprises numerous components with specifically designed and engineered containment properties. The repository itself is embedded in the natural host rock, which consists of a clay formation of substantial thickness that is characterized by low permeability (e.g. Boom clay (ONDRAF), Callo-Oxfordian claystone (ANDRA), Opalinus clay (NAGRA)). Because of its low permeability and low hydraulic gradients, nuclide migration in the host rock is governed mainly by diffusion. The radiological impact of nuclides on the biosphere may be further reduced by radioactive decay and retardation within the repository. Retardation results from complex geochemical reactions, such as surface complexation, inter-layer adsorption and co-precipitation. Due to its favourable properties, the natural host rock is an important component of the safety concept in clay.

#### 3.2 Scenario analysis

Release of  $^{14}\text{C}$  from a clay system is governed by its transport through the disposal system, the containment lifetime (if any) and the dissolution/corrosion rate of the waste form (which could be very slow in an unsaturated system). Because of its relatively short half-life of 5730 years [GODWIN, 1962], the  $^{14}\text{C}$  radiological flux released in the biosphere is particularly sensitive to these processes. For steel and Zircaloy waste, the release rates are so low in expected scenarios that  $^{14}\text{C}$  decays in the waste form before a significant amount is released. The transport parameters are particularly influencing. Indeed, sensitivity analysis show that a decrease in the rate of diffusion of dissolved  $^{14}\text{C}$  by a factor of two through a clay layer of

a few tens of meters thick leads to a reduction of the radioactive flux out of the clay layer by one order of magnitude [Smith, 2014]. Even relatively weak sorption might have a non-negligible effect on the radiological impact.

For scenarios in clay, if  $^{14}\text{C}$  is assumed to be in inorganic form, the typical transport time in clay formation can range from tens of thousands of years to virtually infinity if isotopic exchange with carbonate minerals occurs. This process is well understood and the uncertainties are known.

The importance of the diffusion rate and the impact of the speciation has been highlighted in the studies of NAGRA [KENDALL ET AL., 2015]. A sensitivity analysis has been performed on different factors such as the water flux, the diffusion coefficients, the solubility limits, the sorption coefficients, the dissolution rates of matrix elements and the biosphere dose conversion factors.  $^{14}\text{C}$  from HLW and spent fuel is assumed to be released in organic form. Very specific hypotheses are made for the speciation of  $^{14}\text{C}$  in the ILW and L/ILW depending on the content and the origin of the waste. The results of the scenarios for a HLW repository in the siting region of Zurich Northeast [NAGRA, 2014d, 2014e] show a significant increase of the dose contribution of  $^{14}\text{C}$  only in the case with unfavourable diffusion coefficients (Figure 10). This dose contribution is mainly due to organic species of  $^{14}\text{C}$ . The IRF dominates the  $^{14}\text{C}$  contribution.

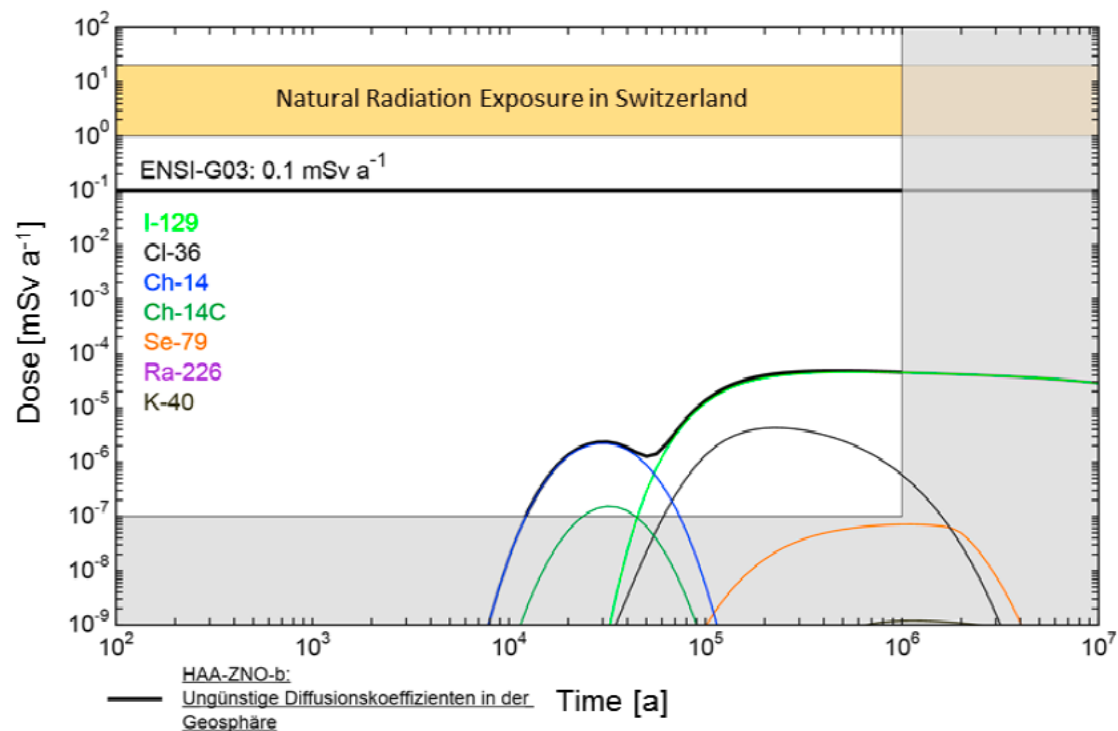


**Figure 10: Dose curve calculated for an HLW repository in the siting Zurich North-east, alternative Case ‘Unfavourable Diffusion Coefficients’ [NAGRA, 2014e, 2014d]. Ch-14 = organic  $^{14}\text{C}$  IRF, Ch- $^{14}\text{C}$  = organic  $^{14}\text{C}$  CR.**

For scenarios, where  $^{14}\text{C}$  is assumed to be mainly in organic form, transport in the gas phase may be important. In this case, safety assessments assume  $^{14}\text{C}$  to be in the form of methane for conservatism. Gas phase transport may lead to accelerated migration of  $^{14}\text{C}$  to the biosphere due to enhanced conductivity and diffusivity (two-phase flow regime) as well as pathway dilation (depending on the geo-mechanical properties of the clay).

Figure 11 and Figure 12 illustrate the treatment of  $^{14}\text{C}$  in safety assessment studies of the CIGEO project [KAEMPFER AND SCHAEDELE, 2016]. Figure 11 indicates the evolution of  $^{14}\text{C}$  concentrations in a deep geological repository and its near-field surrounding. The hydrogen produced by the corrosion of the metallic IL-LL waste fills slowly the engineered system and leads to a desaturated environment for an extended period. Note that corrosion rates have been estimated for saturated environment, however experimental studies carried out on steel embedded in grout by NAGRA [2016] in vapor anoxic conditions suggest also very low corrosion rates of the same order as in saturated conditions. While the amount of hy-

drogen that is generated by anoxic corrosion reaches several billions moles during the simulation period of 1E6 years, only several hundreds of moles of radioactive carbon are generated. The engineered barrier system acts as a gas buffer that allows the gas to dissipate mainly by diffusion through the host rock. Transport times from the Callovo-Oxfordian host rock to the Oxfordian aquifer via the shaft are of the order of tens of thousands of years, and of the order of several hundreds of thousands of years through the host rock. The assessment shows that less than one part per billion of the released  $^{14}\text{C}$  reaches the biosphere environment (Figure 12). The major part (99.99990%) of the released  $^{14}\text{C}$  decays within the disposal site or in its close proximity.

Past safety assessments have shown that advective transport of  $^{14}\text{C}$  (gaseous or aqueous) through a poor sealed system has a limited impact on the outgoing radioactive flux because the advection velocities that can be realistically assumed remain low with respect to the  $^{14}\text{C}$  decay rate, and the pathway through the engineered barrier system is usually longer than the diffusion path through the clay formation (allowing a substantial fraction of  $^{14}\text{C}$  to diffuse in the host rock).

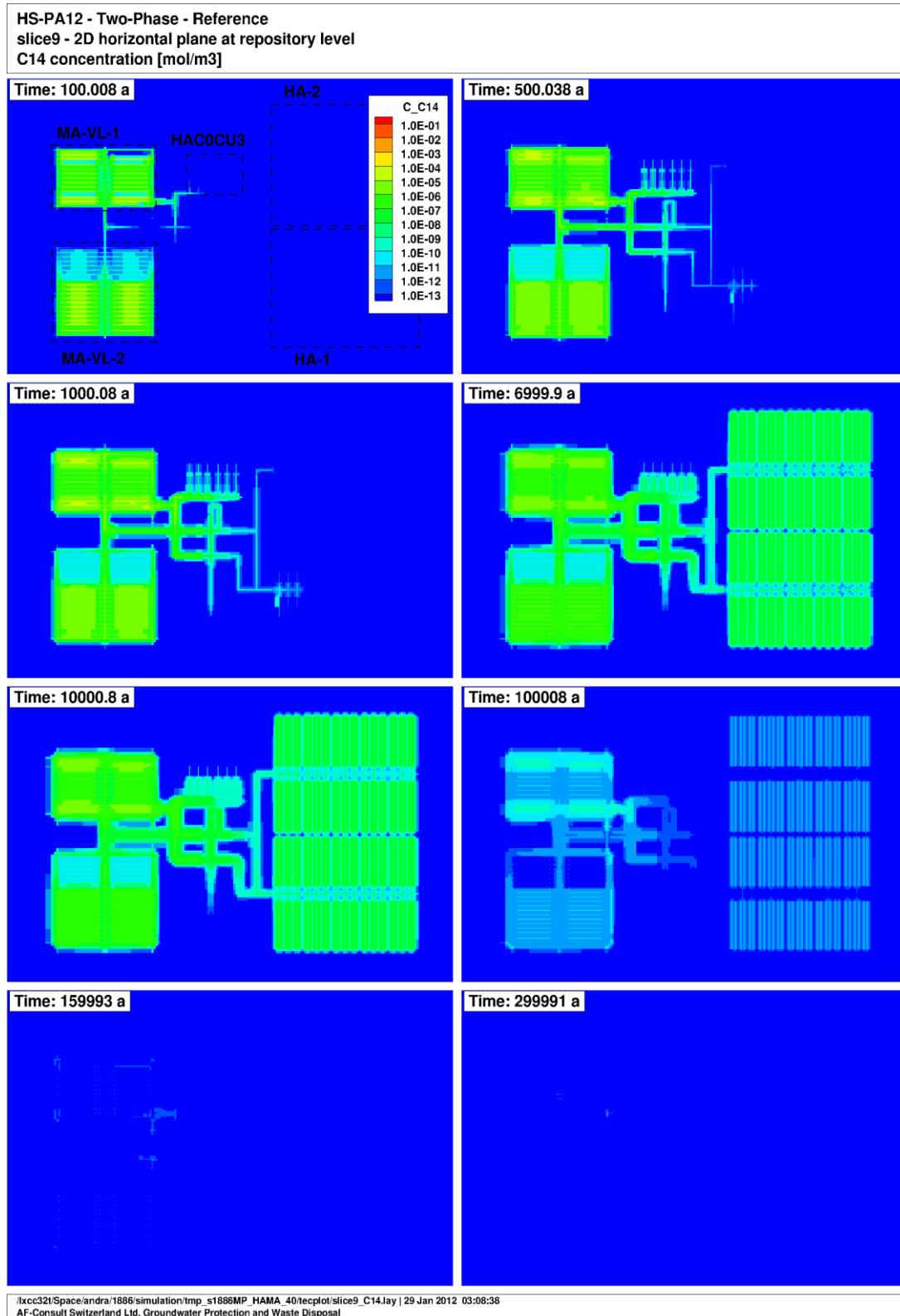
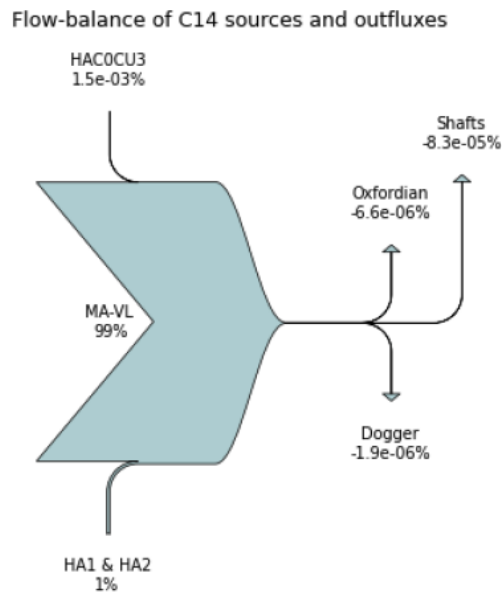


Figure 11: Evolution of  $^{14}\text{C}$  concentrations in the near field of a repository as calculated by the CIGEO project [KAEMPFER AND SCHAEDEL, 2016].



**Figure 12: Mass balance of  $^{14}\text{C}$  as calculated by the CIGEO project [KAEMPFER AND SCHAEDLE, 2016].**

## 4 Safety Assessment in Crystalline Disposal Systems

### 4.1 Safety Concept

The safety concept in crystalline host rock has several components that prevent the release of significant amounts of  $^{14}\text{C}$  to the biosphere. A series of engineered barriers prevent or limit  $^{14}\text{C}$  release into the surrounding host rock. These include the metal and concrete containers, the buffer and backfill (usually made from compacted bentonite or cement) and additional engineered components such as seals and plugs. Although the crystalline host rock itself has less favourable properties with respect to nuclide retention compared to clay disposal systems, reactions with the mineral grains may nevertheless play an important role.

### 4.2 Scenario Analysis

In fractured crystalline rocks, release of  $^{14}\text{C}$  into the biosphere from a repository is mainly governed by migration along fracture networks (Figure 13). The relatively fast groundwater flow might transport  $^{14}\text{C}$  into biosphere prior to any significant decay once released from the engineered barriers. Therefore, the  $^{14}\text{C}$  release rate to the biosphere is mainly governed by the release from the waste disposed system and transport through the engineered barriers.

Hence, the structural repository components such as the concrete containment have an important impact on the overall repository performance.

The fast transport of  $^{14}\text{C}$  in crystalline host rock is illustrated by Figure 14, which shows the annual doses arising from  $^{14}\text{C}$  released from spent ion-exchange resins and activated steel parts in a drilled well scenario for Loviisa low and intermediated level waste repository [KENDALL ET AL., 2015]. In this example,  $^{14}\text{C}$  release from activated metal is assumed to be predominantly in organic form and retention in concrete is not accounted for (or only in a marginal way).  $^{14}\text{C}$  is amongst the most important contributors to radiological dose at the surface immediately above a repository. The evolution of the pH due to aging of the concrete material might lead to increasing release rates provided pH is so low that metal corrosion becomes active. As long as the cementitious environment remains in phase 1&2, passivation should be ensured. The effect of a loss of alkalinity is captured in Figure 14 of the safety assessment carried out by FORTUM [EURAJOKI, 2008; EURAJOKI, 2006]. Results show that the increase of  $^{14}\text{C}$  due to the loss of alkaline conditions remains limited because  $^{14}\text{C}$  has largely decayed after a few tens of thousands years. For waste type like the solidified waste whose release in safety assessment relies entirely on the performance of the concrete barriers, the radiological impact occurs much faster and is, consequently, potentially higher since the radiological activity has not much decayed.

Even more rapid transport of  $^{14}\text{C}$  could occur if it is transported as gas through engineered barriers and host rock, but as the advective transport is relatively fast, the effect of gas transport may not considerably alter the release rate. However, this might differ between different repositories.

The contributions of different waste materials to the overall dose rate assessed by RWMC [KENDALL ET AL., 2015] is given in Figure 15. The figure shows the significant contribution of the hull oxides, because they are assumed to be released instantaneously (IRF).

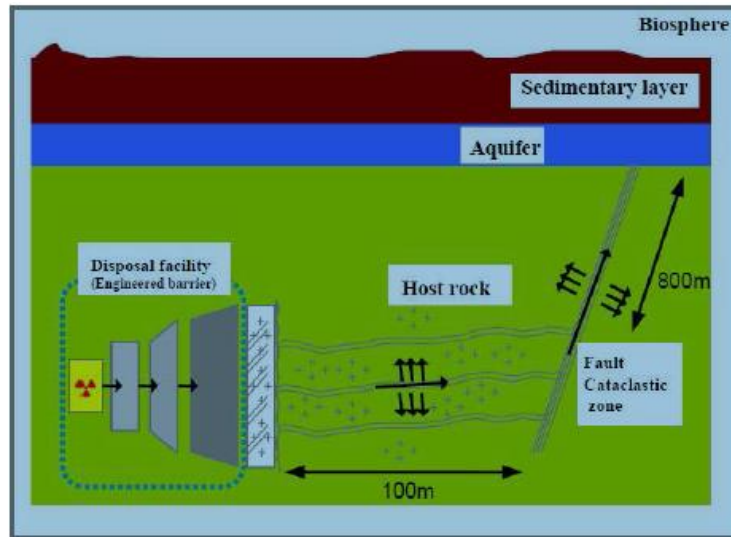


Figure 13: Transport paths in crystalline host rock [JAEA AND FEPC, 2007].

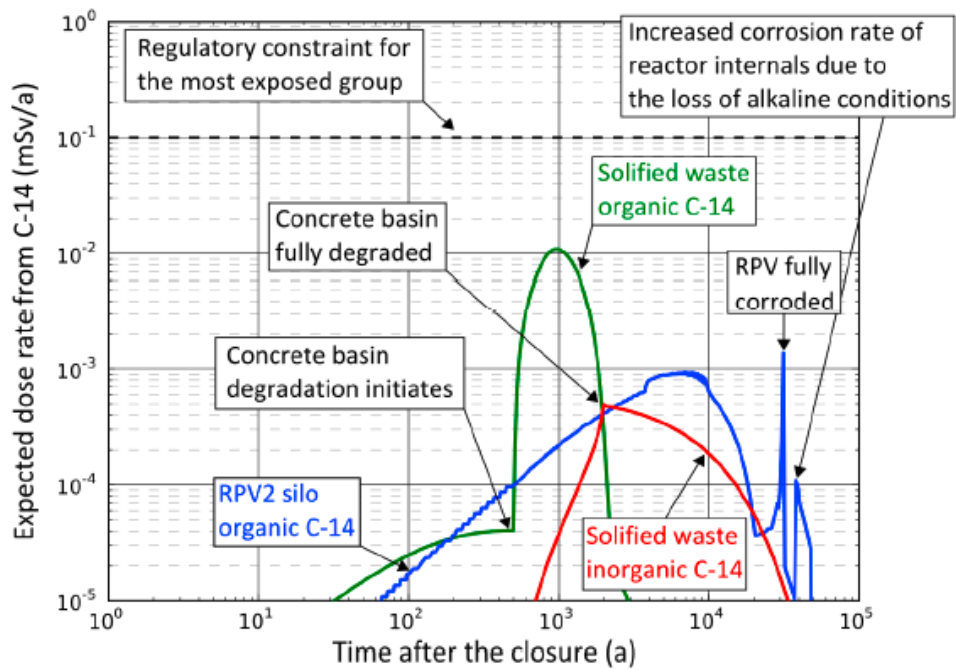
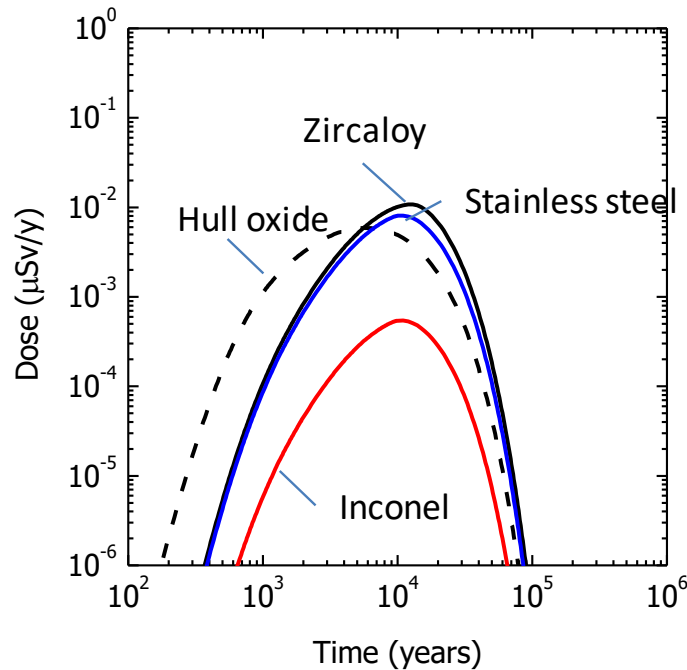


Figure 14: Expected dose rate for the base case scenario of the Loviisa repository with conservative parameter values [EURAJOKI, 2008; EURAJOKI, 2006].



**Figure 15: Contribution of different waste materials to the overall dose rate as calculated by JAEA AND FEPC [2007] and SAKURAGI ET AL. [2013].**

## 5 Safety Assessment in Salt Disposal Systems

### 5.1 Safety Concept

In salt disposal systems, unsaturated conditions persist until the end of the assessment period. A fundamental aspect of the safety concept in salt is the convergence of the caverns, shafts and drifts due to the plasticity of the salt host rock. Convergence leads to the reduction of permeability (can be as low as  $10^{-20} \text{ m}^2$ ) and porosity, which ensures the isolation of the waste and prevents nuclide migration by sealing transport pathways. The emplacement chambers and drifts are backfilled with dry salt grit and sealed with concrete. Non-compactable backfill material in infrastructure sections provides pore space for gas storage. In essence, concrete components provide short-term isolation and compacted salt grit provides long-term isolation.

### 5.2 Scenario Analysis

In the reference scenario for the salt disposal system in Gorleben, GRS postulates that a lifetime of a few hundred years is assumed for the carbon steel waste containers, with the

exception of a small number of containers with initial defects at the time of emplacement. A flow of non-radioactive gases starts in the mine at the beginning of the post-closure phase. This is due to the convergence of the salt host rock and the decreasing porosity in the salt grit used as backfill. Additionally, a hydrogen flow results from the iron corroded by the small amount of water initially emplaced with the containers. The <sup>14</sup>C instantaneously mobilised from the IRF of the Zircaloy is assumed to be released in the form of CO<sub>2</sub> from the initially defect spent fuel containers and is transported along with the non-radioactive gases through the unsaturated drifts. IRF is the most, if not the only contributor to the radiological impact. Should dissolved <sup>14</sup>C be released through the drifts and the shaft, the characteristic diffusive transport times exceed 10<sup>5</sup> years [LARUE ET AL., 2013].

The reference scenario calculated by GRS is shown in Figure 16. The early peak is related to the small number of containers assumed to already have a defect at the time of emplacement. An additional peak of the performance indicator value occurs after about 10<sup>4</sup> years. This peak results from the majority of containers failing after a few hundreds of years. The parameter variations, which are displayed on the figure account for the uncertainty of the location of the initial defect containers within the mine, the corrosion rate of metal parts and the humidity in the containers. The safety assessment simulations summarized here show that <sup>14</sup>C in the gas phase is the most relevant radionuclide.

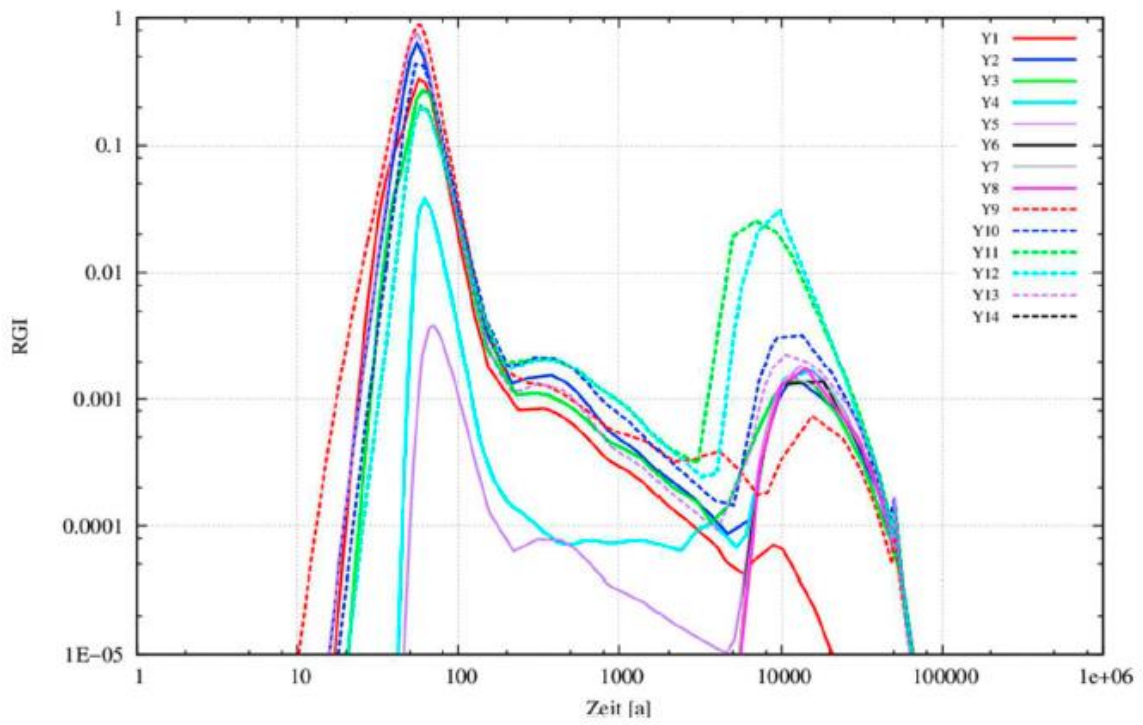


**Figure 16: Performance indicator (RGI) resulting from the  $^{14}\text{C}$  flux out of the spent fuel containers calculated (dimensionless unit) [LARUE ET AL., 2013].**

## 6 Conclusions

The review of the literature undertaken in the first steps of CAST as well as the preliminary experimental results reveal the presence of a non-negligible fraction of organic  $^{14}\text{C}$  compounds in the four waste materials investigated.

First experimental results of leaching tests on steels indicate the presence of small oxygenated species. The formation mechanism is under investigation and it is too early to abstract these observations in safety assessment hypothesis or safety cases argumentation. However, the literature review confirms the very low corrosion rates for steel in reducing conditions. On this basis, it can be expected that an important amount of  $^{14}\text{C}$  will decay in the material before it can be released.

A very good knowledge has been acquired on the  $^{14}\text{C}$  inventory in Zr cladding allowing for a more realistic estimation. Similarly, to steel, corrosion rates are very low in reducing conditions and organic released products have been identified. The main uncertainties point to the instant release fraction of particular importance in safety assessment. Traditionally a value between 10 and 20% is considered for  $^{14}\text{C}$  in Zy-4 based on a homogeneous distribution of  $^{14}\text{C}$  in the cladding and a full release of the total amount of  $^{14}\text{C}$  present in the oxygenated layer. However, experimental observations indicate a much lower  $^{14}\text{C}$  release from the oxidized layer. Further analyses are required to clarify whether these measurements are representative of an instant release fraction fit for safety assessment.

SIERs provide a more heterogeneous picture. Operational and storage conditions as well as conditioning processes influence the  $^{14}\text{C}$  content in the final waste form. First results in CAST from two leaching experiments from EDF resins (PWR) give reproducible results with 77 % of the total  $^{14}\text{C}$  in mineral form and the complement in organic form (23%). No discussions have been initiated yet on the transferability of these results.

$^{14}\text{C}$  leached from irradiated graphite under alkaline conditions is in hydrocarbon/organic forms as well as inorganic ( $^{14}\text{CO}_2$ /carbonate) forms. Only a relatively small proportion of the  $^{14}\text{C}$  is released in laboratory experiments. The proportion of inorganic compounds reported by different sources vary from 20% to 65–75%. Gas phase releases include both vol-

atile  $^{14}\text{C}$ -hydrocarbon/organics (probably  $^{14}\text{CH}_4$ ) and  $^{14}\text{CO}$  but it is a small proportion of the total  $^{14}\text{C}$  released. The release from irradiated graphite  $^{14}\text{C}$  compounds and the ratio between organic/inorganic fraction is under investigation in CAST.

Due to its relatively short half-life, the  $^{14}\text{C}$  radiological flux is sensitive to parameterization of release and migration processes through the disposal system. A reduction of uncertainties pertaining to instant release fraction might have discernable effect. Also, assigning a weak retention to  $^{14}\text{C}$  organic compounds in safety assessment could be beneficial. However, a robust modeling of this retention will depend on the degree of knowledge on  $^{14}\text{C}$  speciation (e.g. detailed speciation or classification by functional chemical groups) and the characteristic of the sorbing solids (e.g. degradation state of the cement, clay characteristics). The source term of the exchange ions resins is determined by the cement degradation in safety assessment studies. Knowledge of the cement evolution is thus important.

Next stage in CAST WP6 will focus on modelling development including sensitivity/uncertainty analysis of parameters and processes associated to  $^{14}\text{C}$  fate in disposal system such as  $^{14}\text{C}$  speciation, retention processes in clay and cement, instant release fraction vs. congruent release and inventory.

## References

- ALLEN, KONINGS, AND MOTTA, 2012. Corrosion of Zirconium alloys. *Comprehensive Nuclear Materials*. VOLUME 5, PP. 49-68.
- AMSTERDAM: ELSEVIER.EC, 2016. Carbon-14 Project Phase 2. Irradiated Graphite Wastes. *AMEC for Radioactive Waste Management Limited*, RP50, AMEC/200047/004 Issue 2.
- AMEC, 2016. Carbon-14 Project Phase 2. Irradiated Graphite Wastes. *AMEC for Radioactive Waste Management Limited*, RP50, AMEC/200047/004 Issue 2.
- AMEC, 2014. Carbon-14 Release from Oldbury Graphite. NPO004819, AMEC/5352/002 Issue 3.
- ANDRA, 2005. Tome: Phenomenological evolution of a geological repository. *Agence Nationale pour la Gestion des Déchets Radioactifs (Andra)*, Dossier 2005 Argile, Report series.
- BARTAGNON, 2003. Residus Vitrifiés La Hague – Inventaire Radioactif. Note Technique NT/0083 53/VEL/03.00001-Rev1.
- BORDIER, 2008. Division Combustible Nucléaire. *EDF*, private communication.
- BOULANGER, LIPPENS, AND POTTEN, 2005. Characterization of Irradiated Fuel Assembly - Part 2 : Assembly behaviour after irradiation. Belgonucleaire report Technical note 0301059/740-D.
- BUCUR, COMTE, LEGRAND, RIZZATO, RIZZO, VEČERNÍK, AND REILLER, 2015. 2nd Annual progress report on WP4. CAST report D4.3.
- CARUSO, MELESHYN, AND NOSECK, 2015. Estimation and comparison of the radionuclide inventories in vitrified high-level wastes from reprocessing plant. *Progress in Nuclear Energy*, in press. doi:10.1016/j.pnucene.2015.11.003
- CATHERIN, PETIT, AND COMPTE, 2016. Carbon-14 Speciation in Solution and Gas from French Graphite Waste. *ANDRA, EDF, CEA, CAST* report D.5.8.
- CHU, WU, AND KUO, 2008. Hydride reorientation in Zircaloy-4 cladding. *Journal of nuclear materials* 373 (2008) 319-327.
- CROZET, PEYRILLOUS, ESBELIN, GARNIER, AND RANDON, 2016. Measurement of  $^{14}\text{C}$  in spent fuel: use of ozone. *Journal of Radioanalytical and Nuclear Chemistry*, 307, 347–353. doi:10.1007/s10967-015-4279-y
- DEHAUDT, DUBOIS, MAGUIN, HUET, PELLETIER, LACROIX, PASQUET, GUÉRIN, HOURDEQUIN, SALOT, DESGRANGES, DELETTE, AND STRUZIK, 2000. Le combustible nucléaire et son état

physico-chimique à la sortie des réacteurs. *CEA Saclay, Direction de l'information scientifique et technique*, CEA-R-5923.

EPRI, 2010. Estimation of Carbon-14 in Nuclear Power Plant Gaseous Effluents. *Electric Power Research Institute (EPRI)*, Technical Report 1021106.

EURAJOKI, 2008. Loviisa NPP Safety Case for the Final Disposal of the Decommissioning Waste. *Fortum Nuclear Services Oy, Espoo, Finland*, Report TJATE-G12-114.

EURAJOKI, 2006. Loviisa Low and Intermediate Level Waste Repository, Safety Case. *Fortum Nuclear Services Oy, Espoo, Finland*, Report LOKIT-5243.

FERRY, PIRON, POULESQUEN, AND POINSSOT, 2008. Radionuclides Release From the Spent Fuel Under Disposal Conditions: Re-evaluation of the Instant Release Fraction. *MRS Proceedings*, 1107, 447–454. doi:10.1557/PROC-1107-447

GEBHARDT AND GOLL, 2012. Characteristic of Spent Nuclear Fuel. *Presented at the 1st Annual Workshop Proceedings of the Collaborative Project "Fast/Instant Release of Safety Relevant Radionuclides from Spent Nuclear Fuel,"* KIT Scientific Publishing, Budapest, Hungary.

GODWIN, 1962. Half-life of Radiocarbon. *Nature*, 195, 984–984. doi:10.1038/195984a0

GRAS, 2014. State of the art of  $^{14}\text{C}$  in Zircaloy and Zr alloys -  $^{14}\text{C}$ -release from zirconium alloy hulls. *Agence Nationale pour la Gestion des Déchets Radioactifs (Andra)*, CAST report D3.1.

GUENTHER, BLAHNIK, THOMAS, BALDWIN, AND MENDEL, 1990. Radionuclide distribution in LWR spent fuel. *Presented at the Nuclear and Hazardous Waste Management International Topical Meeting*, Pacific Northwest Laboratory, Knoxville, Tennessee.

IAEA, 2009. Quantification of Radionuclide Transfer in Terrestrial and Freshwater Environments for Radiological Assessments. *International Atomic Energy Agency (IAEA)*, IAEA-TECDOC-1616.

IAEA, 2006. Characterization, Treatment and Conditioning of Radioactive Graphite from Decommissioning of Nuclear Reactors. *International Atomic Energy Agency (IAEA)*, IAEA-TECDOC-1521.

IAEA, 2004. Management of Waste Containing Tritium and Carbon-14. Technical Report Series No. 421.

IAEA AND FEPC, 2007. Second Progress Report on Research and Development for TRU-Waste Disposal in Japan. *Japan Atomic Energy Agency, The Federation of Electric Power Companies of Japan*, IAEA-Review 2007-010, FEPC TRU-TR2-2007-01.

JOBAGY, DRUYTS, SAKURAGI, FULGER, BUCUR, AND BOTTOMLEY, 2015. Annual progress report on corrosion test. *SCK•CEN, RWMC, RATEN ICN, JRC-ITU*, CAST Report D3.10.

JOHNSON, FERRY, POINSSOT, AND LOVERA, 2005. Spent fuel radionuclide source-term model for assessing spent fuel performance in geological disposal. Part I: Assessment of the instant release fraction. *Long Term Evolution of Spent Nuclear Fuel - A selection of papers from the Spent Fuel Workshop 2004*, 346, 56–65. doi:10.1016/j.jnucmat.2005.04.071

JOHNSON AND TAIT, 1997. Release of segregated nuclides from spent fuel. *Svensk kärnbränslehantering AB/Swedish Nuclear Fuel and Waste Management*, Technical Report TR 97-18.

KAEMPFER AND SCHAEDELE, 2016. Le Transitoire Hydraulique-Gaz pour l'Architecture Japs03b de CIGEO a Fin 2014. *AF-Colenco AG Baden, Schweiz*, Rapport ANDRA CCRPFEAP160036.

KENDALL, CAPOUET, BOULANGER, SCHUMACHER, WENDLING, GRIFFAULT, DIACONU, BUCUR, RÜBEL, FERRUCCI, LEVIZZARI, LUCE, SAKURAGI, TANABE, NUMMI, POSKAS, NARKUNIENE, GRIGALIUNIENE, GRUPA, ROSCA-BOCANCEA, MEEUSSEN, VOKÁL, KÄLLSTRÖM, CUÑADO PERALTA, MIBUS, AND PANTELIA GARCÉS, 2015. Handling of C-14 in current safety assessments: State of the art. *RWM, ONDRAF/NIRAS, ANDRA, RATEN ICN, GRS, ENEA, RWMC, FORTUM, LEI, NRG, SURAO, SKB, ENRESA, NAGRA*, CAST Report D6.1.

LARUE, BALTES, FISCHER, FRIELING, KOCK, NAVARRO, AND SEHER, 2013. Radiologische Konsequenzenanalyse. Bericht zum Arbeitspaket 10. Vorläufige Sicherheitsanalyse für den Standort Gorleben. *Gesellschaft für Anlagen- und Reaktorsicherheit*, GRS-289.

MIBUS, SWANTON, SUZUKI-MURESAN, RODRIGUEZ ALCALA, LEGANÉS NIETO, BOTTEMLEY, HERM, DE VISSER-TYNOVA, CVETKOVIC, SAKURAGI, JOBBAGY, AND HEIKOLA, 2015. WP2 Annual Progress Report: Year 2. CAST Report D2.5.

NAGRA, 2016. Understanding and Quantifying the Corrosion of Carbon Steel in Grouts relevant to the Swiss L/ILW Repository. *Nationale Genossenschaft für die Lagerung radioaktiver Abfälle (NAGRA)*, Nagra Working Report NAB 15-17.

NAGRA, 2014a. Scientific basis for the production of gas due to corrosion in a deep geological repository. *Nationale Genossenschaft für die Lagerung radioaktiver Abfälle (NAGRA)*, Nagra Working Report NAB 14-21.

NAGRA, 2014b. Geochemische Nahfeld-Daten zu den SMA und ATA für die provisorischen Sicherheitsanalysen in SGT Etappe 2. *Nationale Genossenschaft für die Lagerung radioaktiver Abfälle (NAGRA); Paul Scherrer Institut (PSI)*, Nagra Working Report NAB 14-52.

NAGRA, 2014c. A model for radionuclide release from spent UO<sub>2</sub> and MOX fuel. *Nationale Genossenschaft für die Lagerung radioaktiver Abfälle (NAGRA)*, Nagra Working Report NAB 13-37.

NAGRA, 2014d. Provisorische Sicherheitsanalysen für SGT Etappe 2: Elektronischer Daten- und Resultateordner (EDR). *Nationale Genossenschaft für die Lagerung radioaktiver Abfälle (NAGRA)*, Nagra Working Report NAB 14-36.

NAGRA, 2014e. SGT Etappe 2: Vorschlag weiter zu untersuchender geologischer Standortgebiete mit zugehörigen Standortarealen für die Oberflächenanlage: Charakteristische Dosisintervalle und Unterlagen zur Bewertung der Barrierensysteme. *Nationale Genossenschaft für die Lagerung radioaktiver Abfälle (NAGRA)*, Nagra Technical Report NTB 14-03.

NAGRA, 2016. Understanding and Quantifying the Corrosion of Carbon Steel in Grouts relevant to the Swiss L/ILW Repository. *Nationale Genossenschaft für die Lagerung radioaktiver Abfälle (NAGRA)*, Nagra Working Report NAB 15-17.

NDA, 2016. Geological Disposal. Carbon-14 Project Phase 2: Overview Report. *Nuclear Decommissioning Authority (NDA)*, NDA Report NDA/RWM/137.

ONDRAF/NIRAS, 2008. Evolution of the Near-Field of the ONDRAF/NIRAS Repository Concept for Category C Wastes. *Galson Sciences Ltd for ONDRAF/NIRAS*, First Full Draft Report NIROND-TR 2007-07E.

REILLER, BUCUR, COMTE, HEISBOURG, LEBEAU, RIZZATO, RIZZO, AND VEČERNÍK, 2014. Annual progress report on WP4. CAST Report D4.2.

RIZZATO, RIZZO, HEISBOURG, VEČERNÍK, BUCUR, COMTE, LEBEAU, AND REILLER, 2015. State of the art review on sample choice, analytical techniques and current knowledge of release from spent ion-exchange resins. CAST Report D4.1.

SAKURAGI, TANABE, HIROSE, SAKASHITA, AND NISHIMURA, 2013. Estimation of Carbon 14 Inventory in Hull and End-Piece Wastes from Japanese Commercial Reprocessing Operation. *Presented at the 15th International Conference on Environmental Remediation and Radioactive Waste Management*, Proceedings of the ASME, American Society of Mechanical Engineers, Brussels, Belgium.

SAKURAGI, YOSHIDA, KATO, AND TATEISHI, 2016. Study of stainless steel corrosion by hydrogen measurement under deoxygenated, low-temperature and basic repository conditions. *PROGRESS IN NUCLEAR ENERGY*, 87.

SHOESMITH AND ZAGIDULIN, 2011. The corrosion of zirconium under deep geologic repository conditions. *Journal of Nuclear Materials*, 418, 292–306.  
doi:10.1016/j.jnucmat.2011.07.028

SKB, 2010. Data report for the safety assessment SR-Site. SKB TR-10-52.

SKB, 2005.  $^{14}\text{C}$  produced in Swedish nuclear power reactors – measurements on spent ion exchange resins, various process water systems and ejector off-gas. SKB R-05-78.

SMART, FENNEL, RANCE, REDDY, AND NIXXON, 2014. Experimental Studies of Radiation-Induced Corrosion in Support of The Belgium Supercontainer Concept. AMEC Report.

SMITH, 2014. Near Field and geosphere parameter sensitivity analyses for the Reference Scenario in support to SFC1. Project Report NPB 14-12.

SWANTON, BASTON, AND SMART, 2015. Rates of steel corrosion and carbon-14 release from irradiated steels - state of the art review. AMEC, CAST Report D2.1.

TOULHOUT, NARKUNAS, ZLOBENKO, DIACONU, PETIT, SCHUMACHER, CATHERIN, CAPONE, LENZA, PIÑA, WILLIAMS, FACHINGER, AND NORRIS, 2015. Review of Current Understanding of Inventory and Release of C14 from Irradiated Graphite. CAST Report D.5.5.

VAN KONYNENBURG, 1992. Carbon-14 Releases. *Presented at the Nuclear Waste Technical Review Board: Full Board Meeting*, Lawrence Livermore National Laboratory (LLNL), Las Vegas, Nevada.

VERHOEF, NEEFT, DEISSMANN, FILBY, WIEGERS, AND KERS, 2016. Waste families in OPERA. OPERA, OPERA-PG-COV023.

YAMAGUCHI, TANUMA, YASUTOMI, NAKAYAMA, TANABE, KATSURAI, KAWAMURA, MAEDA, KITAO, AND SAIGUSA, 1999. A study on chemical forms and migration behavior of radionuclides in hull wastes. *Presented at the ICEM*, Nagoya, Japan.

## Appendix 1

**Table A: <sup>14</sup>C inventory for different waste types [KENDALL ET AL., 2015].**

Waste type	Waste origin	<sup>14</sup> C inventory	N impurity content (ppm)	Source of data	Reference
Fuel assembly	PWR-BWR: 35-65 GWd/tHM	20-125 GBq/tHM	Fuel: 15-75 Zr alloy: 40-80 SS: up to 1300	ORIGEN-S; OR-EST; Literature	ENRESA; GRS; ONDRAF; NAGRA; SKB
	WWR: 20-60 GWd/tHM	10-235 GBq/tHM	Fuel: 30-200 Zr alloy: 30-75	OREST; N impurities: pessimistic assumptions	GRS; SURAO
	CANDU: 7.5 GWd/tHM	6-20 GBq/tHM	NA	Canadian estimation based on ORIGEN	RATEN
Zr alloy	LWR cladding	0.03-0.08 GBq/kg	30-80	<sup>14</sup> C: ORIGEN-S/ARP N: Literature	ANDRA; ENRESA; ONDRAF; RWMC; NAGRA
	CANDU pressure tube	1.5 GBq/kg		<sup>14</sup> C: Canadian estimation based on ORIGEN	RATEN
	CANDU Zy-4		10-40	N:Measurements	RATEN
Steel	LWR assembly structural parts	0.1-0.4 GBq/kg	400-1300	<sup>14</sup> C: ORIGEN-S/ARP N: Literature	ENRESA; ONDRAF; RWMC; NAGRA
	LWR core internals	< 0.7 GBq/kg	90-1000	<sup>14</sup> C MCNP/3-D; ORIGEN-S N:Measurements	ONDRAF; SURAO; NAGRA; SKB
	LWR core internals	0.4 GBq/kg	400-1400	[EURAJOKI, 2008]	FORTUM
	LWR pressure vessel	< 0.02 GBq/kg	50-100	<sup>14</sup> C: MCNP/3-D N: Measurements	FORTUM; SKB; NAGRA
	LWR pressure vessel	0.003 GBq/kg	400-1400	[EURAJOKI, 2008]	FORTUM
IER	Reactor coolant	0.001 GBq/kg		Measurements	FORTUM
	LWR	0.002 – 0.01 GBq/kg		Measurements	NAGRA
	PWR condensate clean up resins/reactor coolant clean-up	0.001 GBq/kg		Measurements	SKB
	PWR coolant	0.005 GBq/kg		Estimates	ONDRAF
		0.00013 GBq/kg		Measurements	SURAO

Waste type	Waste origin	<sup>14</sup> C inventory	N impurity content (ppm)	Source of data	Reference
	PWR coolant	0.0001-0.001 GBq/kg		Measurements	ANDRA
	Processed together with sludge. Aggregated origin from nuclear power plant	7.1 GBq/waste package (conditioned waste)		Validated ANDRA scaling factor used to determine carbon-14 content from reported cobalt-60 content [IAEA, 2009].	COVRA ([VERHOEF ET AL., 2016])
Graphite	TRIGA	10 <sup>-5</sup> -10 <sup>-2</sup> GBq/kg		Measured	RATEN
	RBMK	~ 1 GBq/kg	70	Activation: ORIGEN-S, N: Literature	LEI
		0.01-0.1 GBq/kg		Computation and radiochemical measurements	ANDRA
CSD-V	47 Gwd/tHM	11 GBq/package		Function of the carry-over fraction from the reprocessing cycle	ONDRAF
	33 GWd/tHM	17.9 GBq/package			GRS
	33-45 GWd/tHM	~3 GBq/package			ANDRA
		1-3 GBq/package			NAGRA
CSD-C	- 47 GWd/tHM	45 GBq/package	Zr alloy: 80 Steel: 1000		ONDRAF
	- 33 GWd/tHM	13.8 GBq/package	45-75	OREST simulation; N impurities: pessimistic assumptions	GRS
	~60 GWd/tHM	~20 GBq/package	30-40	Measurement (tritium tracer); Modelling CESAR	ANDRA
		15 GBq/package	Zr: 70-80 Steel: 400-800	<sup>14</sup> C: Declaration of producer + Burnup calculation (ORIGEN-S/ARP) N: Literature	NAGRA
	515 MW <sub>e</sub>	13.8 GBq/package		Declaration AREVA, 2001	COVRA ([VERHOEF ET AL., 2016])

## Appendix 2

### List of references for figure 3

Van Konynenburg R.A., 1994. Behavior of Carbon-14 in Waste Packages for spent Fuel in a Tuff Repository. Waste Management, Vol. 14, No. 5, pp. 363-383 – 1994.

Marimbeau P. et al., N and C-14 contents of spent fuel. 2003 NAGRA-RWMC - Workshop on C14 release and transport in repository environments.

de Wouters R. Characterisation of Irradiated Fuel Assemblies: Radionuclide Inventory in Spent Fuel Elements. BELGATOM report 0204246/221, June 2003.

Bleier A. et al., 1987. Carbon-14 Inventories and behaviour in LWR-Spent Fuel Rods During Reprocessing. Proc. Internat. Conf. on Nuclear Fuel Reprocessing and Waste Management “Recod 87”, Vol. 3, p.1089-1094.

Roddy J.W. et. al., Physical and Decay Characteristics of Commercial LWR Spent Fuel. Oak Ridge National laboratory report ORNL/TM-9591 /V1&R1

Guenther R.J. et al., 1994. Radiochemical Analyses of Several Spent Fuel Approved Testing Materials Pacific Northwest Laboratory report PNL-10113/UC-802.

Naegeli R.E., 2004. Calculation of the Radionuclides in PWR Spent Fuel Samples for SFR Experiment Planning. Sandia National Laboratories report SAND2004-2757.

Jubin R.T. et al., 2010, Control of Volatile Radionuclides from the Dissolution of Used Nuclear Fuel – 10224. WM2010 Conference, Phoenix.

Roque B. et al. 2013. International Comparison of a Depletion Calculation Benchmark on Fuel Cycle Issues - Results from Phase 1 on UOx Fuels. NEA report NEA/NSC/DOC(2013)1.

References from CAST D3.1 :

Laugier F., 2003. Inventaire radiologique et thermique des assemblages REP usés : combustible UOX 4.95 %, EDF R&D Technical Report HI-28/2003/022-A, June 2003.

Sakuragi T. et al. 2013. Estimation of carbon 14 inventory in hull and end piece wastes from Japanese commercial reprocessing operation, ASME 2013 15th International Conference on Environmental Remediation and Radioactive Waste Management, ICEM2013, 8-13 September 2013, Brussels, Belgium, Paper n°96110.

Smith H.D. & Baldwin D.L.1993. An investigation of thermal release of carbon-14 from PWR Zircaloy spent fuel cladding. J. of Nuclear Materials 200, 128-137.

### Appendix 3

A WP6 technical meeting was organised in Wetingen (Switzerland) at the NAGRA offices in March 2016. The focus of the first day was on the preliminary integration of CAST results in WP6. This meeting took place in the framework of task 6.2. Following the CAST workplan, a one-day meeting was held in order to challenge safety assessment treatments of  $^{14}\text{C}$  in current safety cases and formal safety assessments (reported in D6.1) with the knowledge base on  $^{14}\text{C}$  release (reported in D2.1, D3.1, D4.1 and D5.5) and the preliminary experimental results. For this purpose, Work package leaders of WP2, 3, 4 and 5 participated to this technical meeting.

The thematic areas of the second day were on : 1/ Speciation & chemical behaviour along the transport pathway in clay, salt and cementitious environment of a disposal system, 2/  $^{14}\text{C}$  instant release fraction and 3/  $^{14}\text{C}$  transfer in the biosphere were also discussed.

Abstracts over the FIRST-Nuclides project and over the chemical interactions of  $^{14}\text{C}$  -bearing compounds in salt conditions were provided by B. Kienzler (INE/KIT). E. Wieland and L. Van Loon from PSI gave a presentation on “Retention of low molecular weight organics in a cementitious environment” and “Fate of  $^{14}\text{C}$  –bearing compounds in clay”, respectively. R. Walke from Quintessa presented progress made on  $^{14}\text{C}$  in the BIOPROTA project. Their abstracts are included in this appendix.

### ***Retention of low molecular weight organics in a cementitious environment (E. Wieland, PSI)***

A literature survey suggested that small molecules up to C5 are produced during the anoxic corrosion of activated steel in the cementitious near field of a repository for radioactive waste (Wieland & Hummel, 2015). These molecules can carry  $^{14}\text{C}$  and therefore contribute to the dose release from a repository. Some corrosion studies report predominant formation of volatile hydrocarbons, i.e. alkanes and alkenes, while others indicate predominant formation of dissolved, oxygenated hydrocarbons, i.e. alcohols, aldehydes and carboxylic acids. Furthermore, it was noticed that sorption and diffusion studies with low molecular weight (LMW) organics on cementitious materials are scarce. The presentation shows the results from an experimental study on the retention of LMW organics with hardened cement paste (HCP) and cement phases carried out at the Paul Scherrer Institut (Wieland et al., 2016). The study aimed at determining sorption values of some small organic molecules, i.e. methanol, ethanol, formaldehyde, acetaldehyde, formic acid and acetic acid, for use in performance assessment calculations. Preliminary experiments revealed that reliable sorption values can only be determined in compact cementitious systems while measurements in dispersed systems (batch-type sorption studies) were not successful due to the very weak sorption of all compounds except formate. Details of the experimental methods are reported in Wieland et al. (2016). Sorption values of all the above compounds were determined in hydrating compact cement after 1h, 28 d and 390 d ageing. The sorption values determined for formate and acetate were further critically assessed by investigating through- and out-diffusion of these compounds in fully hydrated cement paste and their uptake by individual cement phases. Solid-liquid distribution ratios ( $R_d$  values) determined from the hydration experiments were found to be of the order of  $10^{-4} \text{ m}^3 \text{ kg}^{-1}$  or below in case of alcohols and aldehydes indicating non-specific (very weak) bonding onto the surface of the cement phases, e.g. through hydrogen bonding. Hydration and diffusion studies reveal slightly higher distribution ratios and reversible uptake by HCP and cement phases in the case of acetate indicating specific adsorption (electrostatic interaction) onto partially positively charged surface sites of the cement phases. Selective binding of a small fraction of formate is evidenced from both sorption and out-diffusion experiments suggesting the presence of sorption sites capable of strongly bonding the anion, presumably by  $\text{SO}_4^{2-}/\text{HCOO}^-$  replacement in the ettringite structure. The study clearly shows that, at the pre-

sent time, no compound-specific  $R_d$  values or  $R_d$  values for different classes of organic compounds can be recommended for use in PA due to the limited data set available. Nevertheless, the limited dataset allows a typical  $R_d$  value ( $10^{-4} \text{ m}^3 \text{ kg}^{-1}$ ) (upper bound:  $10^{-3} \text{ m}^3 \text{ kg}^{-1}$ , lower bound:  $10^{-5} \text{ m}^3 \text{ kg}^{-1}$ ) to be recommended for use in PA calculations for all small organic molecules.

## References

Wieland, E., W. Hummel (2015) Formation and stability of carbon-14 containing organic compounds in alkaline iron-water systems: Preliminary assessment based on a literature survey and thermodynamic modelling. *Mineral. Mag.* 79, 1275-1286.

Wieland, E., A. Jakob, J. Tits, B. Lothenbach, D. Kunz (2016) Sorption and diffusion studies with low molecular weight organic compounds in cementitious systems, *Applied Geochem.* 67, 101-117.

*Fate of  $^{14}\text{C}$ -bearing compounds in clay (Y. Chen<sup>1,2</sup>, M. A. Glaus<sup>1</sup>, L. R. Van Loon<sup>1</sup>, U. K. Mäder<sup>2</sup>)*

<sup>1</sup>Laboratory for Waste Management, Paul Scherrer Institut, CH-5232 Villigen PSI, Switzerland

<sup>2</sup> Institute of Geological Sciences, University of Bern, Baltzerstrasse 3, CH-3012 Bern, Switzerland

Organic  $^{14}\text{C}$  species are assumed to be unretarded in current performance assessment scenarios for the far-field of a low- and intermediate-level radioactive waste repository. The transport properties of selected carboxylic acids (CAs) and alcohols in compacted illite, kaolinite and Opalinus Clay (OPA) are being investigated in a running PhD project in order to assess possible weak retardation processes. For this purpose infiltration experiments were carried out on compacted samples of the clay minerals with a fixed confinement or on samples of clay rocks triaxially confined by a pressurized liquid using pulse injections of a single solute or mixtures of solutes of interest.

The pure clay samples (infiltration with NaCl; uncontrolled pH) exhibited symmetrical breakthrough curves with no tailing. Test solutes eluted from illite in the following order:  $^{36}\text{Cl}$ , aliphatic CAs, HTO,  $\beta$ -OH-CAs,  $\alpha$ -OH-CAs [1]. The early breakthrough of  $^{36}\text{Cl}$  suggests an anion exclusion effect caused by the negatively charged illite surface. In kaolinite, the elution order was: HTO, aliphatic CAs,  $^{36}\text{Cl}$ ,  $\beta$ -OH-CAs. Breakthrough curves of all test solutes from OPA (infiltration with artificial pore water;  $\text{Br}^-$  as the reference tracer) were asymmetrical with tailing, which might be caused by the increased predominance of diffusion processes. Compared with  $\text{Br}^-$ , test aliphatic CAs were not retarded in OPA.  $\alpha$ -OH-CAs could not be recovered in the effluents from kaolinite and OPA within the time of observation.

Variations of salinity and pH were conducted in the experiments with pure clay minerals to (i) compare to the OPA system, and (ii) to get further insight into the retardation mechanisms. First results on illite indicated an increasing retardation for all test solutes with increasing salinity. Therefore, the retardation in illite can neither be explained by electrostatic interaction nor ligand exchange. We rather propose that the uptake of the organic test compounds on the

clay surface can be treated formally along the lines of a liquid-liquid phase distribution. Structural features such as the presence of  $\alpha$ -/  $\beta$ -hydroxo group with the metal cations on the clay surface further modify this interaction. The differences between the kaolinite and the illite system suggest that the interaction takes mainly place on octahedral surfaces of the clay minerals.

Correlations between the observed retardation factors and octanol-water distribution coefficients were tested for potential applications of blind-predicting the retardation behavior of unknown organic compounds. A clear correlation could be observed for CA's in illite, while such a correlation was almost absent for the alcohols.

[1] Chen Y, Glaus M.A., Van Loon L, Mäder U (2015) Goldschmidt Abstracts, 2015 527.

### **Chemical interactions of $^{14}\text{C}$ -bearing compounds in salt conditions (B. Kienzler, INE/KIT)**

In the neutron field of nuclear power plants,  $^{14}\text{C}$  is formed by different reactions such as  $^{17}\text{O}(\text{n},\alpha)^{14}\text{C}$ ,  $^{14}\text{N}(\text{n},\text{p})^{14}\text{C}$ ,  $^{13}\text{C}(\text{n},\gamma)^{14}\text{C}$ . The formation by ternary fission is negligible. The final  $^{14}\text{C}$  yield was measured by various investigations of LWR and CANDU fuels and claddings, ranging from 25 MBq/g [1] to 320 MBq/g [2] in the fuel and up to 32 MBq/g Zyr-4 (44 MBq/g Zyr-4 oxide layer) [3].

Depending on the chemical environment after the formation of the heavily charged and excited  $^{14}\text{C}$ , carbonates or metal-carbon compounds (carbides) can be formed. Due to the fact that the mother nuclides are low concentrated, the newly formed metal-carbon compounds may not form carbide crystallites. From thermodynamic considerations, mainly the  $\text{Me}_3\text{C}$  species might be formed. Complex are the chemical interactions of excited carbon with fission products (Mo, Zr, Nb) or with uranium. Mobilization of  $^{14}\text{C}$  from carbides requires the presence of water / salt brines resulting in different hydro carbon phases, for example,  $\text{Al}_4\text{C}_3 \rightarrow \text{CH}_4$ ,  $\text{Mg}_2\text{C} \rightarrow \text{CH}_4$ ,  $\text{CaC}_2 \rightarrow \text{H-C}\equiv\text{C-H}$  or  $\text{Fe}_3\text{C} \rightarrow \text{C}_n\text{H}_{2n+2} + \text{H}_2$ . In the presence of water / salt brines, the gaseous species will be dissolved according Henry's law. These species may undergo abiotic or biotic reactions. The retention of dissolved  $^{14}\text{C}$ -carbonate onto different salt minerals present in German rock salt formations have been investigated and the results have been presented earlier [4].

Well known are thermochemical reactions such as  $\text{CaSO}_4 + \text{CH}_4 \rightarrow \text{CaCO}_3 + \text{H}_2\text{S} + \text{H}_2\text{O}$  which require temperatures  $T > 100^\circ\text{C}$ . Biotic reactions take place below  $100^\circ\text{C}$  oxidize hydrocarbons to  $\text{H}_2$  and  $\text{CO}_2$ , or form methane by  $\text{CO}_2$  reduction. Biotic reactions depend on micro-organisms which are subject to the universal laws saying that matter and energy cannot be destroyed or formed, just transformed. But micro-organisms are utterly sophisticated lawyers that understand to use every single, constructive combination of those laws for making a good living of all or almost nothing [5].

The retention of  $^{14}\text{C}$  in a rock salt disposal In a rock salt disposal can be described as follows: Dissolved carbonate species may precipitate (cement) or be sorbed onto carbonate containing solids (isotopic exchange). Interaction of  $\text{CO}_2$  gas with Mg bearing material leads to the for-

mation of Mg-hydroxo-carbonates and / or magnesite. Weak sorption of  $^{14}\text{CO}_3^{2-}$  onto salt concrete in  $\text{MgCl}_2$ -rich brine was observed and dissolved  $^{14}\text{C}$  was incorporated into solids Sorel phases. The transformation of organic to inorganic  $^{14}\text{C}$  species is extremely slow, however, a potential increase may occur in the presence of microbes, if viable in highly concentrated solutions and under low redox potentials.

#### References

- [1] M.-S. Yim and F. Caron, "Life cycle and management of carbon-14 from nuclear power generation," *Progress in Nuclear Energy*, vol. 48, pp. 2-36, 2006.
- [2] W. SOHN, D.-W. KANG, and W.-S. KIM, "An Estimate of Carbon-14 Inventory at Wolsong Nuclear Power Plant in the Republic of Korea," *Journal of Nuclear Science and Technology*, vol. 40, pp. 604-613, 2003.
- [3] Y. Yamashita, H. Tanabe, T. Sakuragi, R. Takahashi, and M. Sasoh, " $^{14}\text{C}$  Release Behavior and Chemical Species from Irradiated Hull Waste under Geological Disposal Conditions," *MRS Online Proceedings Library*, vol. 1665, pp. 187-194, 2014.

### ***$^{14}\text{C}$ investigations in the scope of FIRST-Nuclides (B. Kienzler, INE/KIT)***

The objective of the Collaborative Project (CP) “Fast / Instant Release of Safety Relevant Radionuclides from Spent Nuclear Fuel (FIRST-Nuclides)” dealt with the understanding of the rapid release of radionuclides from high burn-up  $\text{UO}_2$  (SNF) in deep geological repositories after canister failure. The project intended to obtain information on the relation between the fission gas release and the instant release fraction of the fission products  $^{129}\text{I}$ ,  $^{79}\text{Se}$ ,  $^{135}\text{Cs}$  for high burn-up fuels with relevant linear power rates, and quantification and speciation of the minor components in the fuel, such as  $^{14}\text{C}$  and Se.

The fuels under investigation covered samples from pressure and boiling water reactors with  $^{235}\text{U}$  enrichments between 2.8 and 4.3 %, linear power rating between 143 and 400 W/cm, burn-up between 48 and 70 GWd/ $t_{\text{HM}}$  and fission gas releases between 1.3 and 13.2 %. With respect to the  $^{14}\text{C}$  inventory, calculations were performed taking into account the abundance of the mother isotopes and the thermal and resonance cross sections for the relevant activation reactions  $^{17}\text{O}(n,\alpha)^{14}\text{C}$ ,  $^{14}\text{N}(n,p)^{14}\text{C}$ ,  $^{13}\text{C}(n,\gamma)^{14}\text{C}$ .

For estimation of the potential reaction of the of the heavily charged and excited newly formed  $^{14}\text{C}$  in the  $\text{UO}_2$  fuel, a similar approach was applied which is used in steel production: The decarburization of steel by oxidizing carbon in the metal, preventing simultaneous oxidation of the metal. The relevant reactions depend on the temperature and on the redox state of the fuel during irradiation. The centerline temperatures in a fuel rod as function of the burn-up time and linear power ratings were calculated. At a temperature range  $850 \leq T \leq 1100$  K it could be shown that the free energy of formation  $\Delta G_{\text{CO}/\text{CO}_2} < \Delta G(\text{MoO}_2)$ . In this temperature range  $^{14}\text{CO}/^{14}\text{CO}_2$  species can be formed. Molybdenum may exist in metallic or oxidized form acting as redox buffer in the fuel.

The existence of  $^{14}\text{CO}/^{14}\text{CO}_2$  species were analysed by gas mass spectroscopy in the fission gas sampled from puncturing the plenum of a rod segment of a Gösgen PWR SNF (3.8% init. enrichment, 50 GWd/  $t_{\text{HM}}$ , av. 260 W/cm ). In the fission gas, 7.0 % of total Kr, and 8.5 % of total Xe was found. Following information was obtained: The calculated  $^{14}\text{C}$  mass inventory in the rod segment was  $2.1 \cdot 10^{-4}$  mol, the maximum fraction of  $^{14}\text{CO}_2$  in the fission gas amounted to 0.2 % of  $^{14}\text{C}$  inventory ( $4.3 \times 10^{-6}$  mol).

Within the 3 years duration of the CP FIRST-Nuclides, it was not possible to establish the complete  $^{14}\text{C}$  analytics. KIT, PSI and Studsvik established analytical procedures. The instant release fraction of  $^{14}\text{C}$  by leaching experiments was determined by SCK·CEN, resulting in a cumulative release fraction of 1 to 2 % for clad and declad samples showing no significant increase with time.

## BIOPROTA (R. Walke, Quintessa)

$^{14}\text{C}$  can reach the biosphere in either:

- ▲ the gas phase, via fractured and/or damaged rock, access shafts, access drifts and/or boreholes; or
- ▲ the aqueous phase, via groundwater discharge to surface and/or the use of groundwater via boreholes and wells.

Carbon is a fundamental building block of organic systems and, as such,  $^{14}\text{C}$  requires special consideration when assessing its potential impact in the biosphere. The form of carbon that is released is important. For example, plants are very effective at incorporating carbon dioxide into organic matter via photosynthesis, whereas methane is not taken up as effectively.

For gaseous releases to the atmosphere, dispersion means that inhalation doses are typically low. Some assessments can result in inhalation being an important pathway following geological disposal, however, this depends on very conservative assumptions, including, for example, a house being located directly on top of poorly sealed access shafts (e.g. Penfold et al., 2011).

For gaseous or aqueous releases to surface water, the relatively low carbon content of water, compared with the relatively high carbon content of fish and plants, results in a relatively high degree of apparent uptake. However, rivers typically have a relatively high turnover rate and, for systems with low turnover, like mires and some lakes, then gaseous evasion can be an important loss term.

For gaseous or aqueous releases to the soil, there is a significant degree of potential conversion of methane to carbon dioxide via microbial activity. RWM has undertaken extensive field and laboratory research into the degree of oxidation of methane in soils (e.g. RWM, 2016). This research indicates that  $^{14}\text{C}$  labelled methane reaching the soil from geological disposal may be almost completely converted to  $^{14}\text{C}$  labelled carbon dioxide within a 25 cm depth of agricultural soil.

Isotopic discrimination for  $^{14}\text{C}$  compared to  $^{12}\text{C}$  is relatively small, therefore models for  $^{14}\text{C}$  in the biosphere are typically based on identifying stable carbon ‘pools’ and associated turnover

rates. For long-term releases, ‘specific activity’ assumptions are also adopted, which, for example, assume a consistent ratio between  $^{14}\text{C}$  and stable carbon (expressed as Bq per kg carbon) in the canopy atmosphere and plant tissues, or between water and aquatic plants and fish.

Recent developments in biosphere modelling for  $^{14}\text{C}$  have focused on removing conservatism in the representation of plant uptake by improving the simulation of turbulence within plant canopies based on standard micrometeorological approaches. The [BIOPROTA](#) collaborative biosphere project has provided an international forum for discussing the representation of  $^{14}\text{C}$  in the biosphere and has supported model-model and model-data inter-comparisons (e.g. BIOPROTA, 2015). With the improved models, and for  $^{14}\text{C}$  releases to the soil, the small amount of plant carbon that may be taken up directly from that dissolved in soil water via plant roots and the transpiration stream may be the most important pathway for uptake of  $^{14}\text{C}$  into plants and the food chain (RWM, 2016).

Potential effective doses to humans remain a principal focus of post-closure assessment of the performance of radioactive waste disposal facilities. Assessments will typically also explicitly consider potential impacts on wildlife (both flora and fauna), though wildlife doses are unlikely to be limiting in comparison with potential impacts on humans (e.g. SKB, 2014).

For direct releases to surface water, ingestion of fish can be a dominant exposure pathway (e.g. Walke et al., 2013; Bergström et al., 2008). For releases to land, then ingestion of plant and animal produce are typically important for  $^{14}\text{C}$  (e.g. Penfold et al, 2011). For ingestion of  $^{14}\text{C}$  as bicarbonate or carbon dioxide dissolved in water, recent correspondence indicates that International Radiological Protection Commission ingestion dose coefficients are overestimated by a factor of about forty (Smith and Thorne, 2015; Harrison and Leggett, 2016).

## References

Bergström U, Avila R, Ekström P-A and de la Cruz I (2008). Dose assessments for SFR 1. Svensk Kärnbränslehantering AB (SKB) Report R-08-15, Stockholm, Sweden.

BIOPROTA (2015). Long-term Dose Assessment for Carbon-14: Report of an International Workshop held in Aix-en-Provence 28-30 April 2015. BIOPROTA report Version 2.0.

Harrison J D and Leggett R W (2016). Appropriate selection of dose coefficients in radiological assessments: C-14 and Cl-36: response to the letter of G Smith and M Thorne. *J. Radiol. Prot.* 36 (2) 388.

Penfold J, Garisto N, Janes A, Little R, Ramlakan A, Towler G and Walke R (2011). OPG's Deep Geologic Repository for Low & Intermediate Level Waste - Postclosure Safety Assessment: Analysis of Human Intrusion and Other Disruptive Scenarios. Quintessa and SENES report to the Nuclear Waste Management Organization (NWMO) NWMO DGR-TR-2011-27, Toronto, Canada.

RWM (2016). Geological Disposal. Carbon-14 Project Phase 2: Overview Report. Radioactive Waste Management (RWM) Limited report NDA/RWM/137, Harwell, UK.

SKB (2014). Safety analysis for SFR Long-term safety: Main report for the safety assessment SR-PSU. Svensk Kärnbränslehantering AB (SKB) Technical Report TR-14-01, Stockholm, Sweden.

Smith G M and Thorne M C (2015). Appropriate selection of dose coefficients in radiological assessments: C-14 and Cl-36. *J. Radiol. Prot.* 35 (3) 737–740.

Walke R C, Thorne M C and Limer L M C (2013). RWMD Biosphere Assessment Model: Terrestrial Component. Quintessa and AMEX report to the Nuclear Decommissioning Authority (NDA) Radioactive Waste Management Directorate (RWMD) QRS-1628A-2, Issue 2, Harwell, UK.